05

III

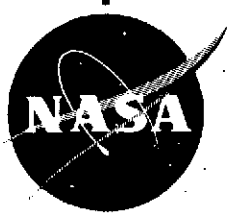

Final Report

REMOTE BATHYMETRY AND SHOAL DETECTION WITH ERTS

ERTS Water Depth - Final Report, Project 193302

FABIAN C. POLCYN and DAVID R. LYZENGA
Infrared and Optics Division

APRIL 1975

Prepared for

NATIONAL AERONAUTICS AND SPACE ADMINISTRATION

Goddard Space Flight Center
Greenbelt, Maryland 20771
Contract NAS5-21783, Task I

1063A

ENVIRONMENTAL
RESEARCH INSTITUTE OF MICHIGAN
FORMERLY WILLOW RUN LABORATORIES, THE UNIVERSITY OF MICHIGAN
BOX 618 • ANN ARBOR • MICHIGAN 48107

NOTICES

Sponsorship. The work reported herein was conducted by the Environmental Research Institute of Michigan for the National Aeronautics and Space Administration, Goddard Space Flight Center, Greenbelt, Maryland 20771, under Contract NAS 5-21783, Task I. E. F. Szajna is Technical Monitor for NASA-GSFC. Contracts and grants to the Institute for the support of sponsored research are administered through the Office of Contracts Administration.

TECHNICAL REPORT STANDARD TITLE PAGE

1. Report No.	2. Government Accession No.	3. Recipient's Catalog No.

4. Title and Subtitle	5. Report Date
REMOTE BATHYMETRY AND SHOAL DETECTION WITH ERTS: ERTS Water Depth — Final Report, Project 193302	April 1975
	6. Performing Organization Code
7. Author(s)	8. Performing Organization Report No.
Fabian C. Polcyn/MMC 063 and David R. Lyzenga	193300-51-F
9. Performing Organization Name and Address	10. Work Unit No.
Environmental Research Institute of Michigan Infrared and Optics Division P.O. Box 618 Ann Arbor, Michigan 48107	Task I
	11. Contract or Grant No. NAS 5-21783
	13. Type of Report and Period Covered Final Report June 1972-June 1974
12. Sponsoring Agency Name and Address	14. Sponsoring Agency Code
National Aeronautics and Space Administration Goddard Space Flight Center Greenbelt Road Greenbelt, Maryland 20771	

15. Supplementary Notes

E.F. Szajna is Technical Monitor for NASA-GSFC.

16. Abstract

Processing algorithms for extracting water-depth information from ERTS data have been developed and applied to two ERTS frames representing different solar-illumination and water-transparency conditions. Depth charts have been produced for these two areas, with a maximum depth of 9 meters under optimum conditions (Little Bahama Bank) and 2 meters under poor conditions (Northern Lake Michigan).

Present processing costs to provide MSS depth charts are estimated to be on the order of $1.50 per square mile. Direct benefits to shipping industries and to agencies responsible for hydrographic charting and erosion control are expected to result from the utilization of these techniques.

17. Key Words	18. Distribution Statement
Remote sensing Bathymetry Shoal detection ERTS Water depth	Initial distribution is listed at the end of this document.

19. Security Classif. (of this report)	20. Security Classif. (of this page)	21. No. of Pages	22. Price
UNCLASSIFIED	UNCLASSIFIED	55	

PREFACE

The general objective of this project was to test the feasibility of using multispectral techniques for the determination of water depths from spacecraft altitudes. Previous research with multispectral aircraft sensors sponsored by the National Oceanic and Atmospheric Agency's Spacecraft Oceanography Group (formerly of the Naval Oceanographic Office), under the direction of John Sherman III, had demonstrated that narrow spectral bands in the blue green portion of the spectrum could be used for remote bathymetry.

This report is submitted in fulfillment of NASA Contract No. NAS5-21783, Task I. The principal investigator on the project was Fabian C. Polcyn, and the work was carried out by the Infrared and Optics Division of the Environmental Research Institute of Michigan under the direction of Mr. R. R. Legault.

The authors wish to acknowledge the contributions of W. L. Brown who worked on the early formulation of the technique and Michael Gordon for assistance in developing the computer programs for this task.

CONTENTS

1. INTRODUCTION 7

2. APPLICATIONS AREA DISCUSSION 8
   2.1 Updating Navigation Charts 8
   2.2 Monitoring Shoreline Changes 10

3. EXTRACTION OF WATER-DEPTH INFORMATION FROM ERTS MSS DATA 10
   3.1 General Considerations 10
   3.2 Single-Channel Method 14
   3.3 Ratio Method 16
   3.4 Optimum Decision-Boundary Method 17
   3.5 Error Reduction by Time-Study Techniques 19

4. DISCUSSION OF RESULTS 20
   4.1 Little Bahama Bank 20
   4.2 Lake Michigan 23

5. EVALUATION OF ERTS POTENTIAL FOR REMOTE BATHYMETRY 40
   5.1 Relative Costs and Accuracies of Remote Sensing Versus Ship Surveys 40
   5.2 Evaluation of ERTS Versus Better Space Sensors for Measuring Water Depth 40

Appendix A: COMPUTER PROGRAM FOR RATIO METHOD 43

Appendix B: COMPUTER PROGRAM FOR OPTIMUM DECISION-BOUNDARY METHOD 50

REFERENCES 54

DISTRIBUTION LIST 55

FIGURES

1. MSS Output Count (V_i) Versus Radiance (R_i/R_{max}), Compressed and Linear Modes 13
2. Geometry of Water-Depth Measurement 13
3. Attenuation Coefficient Versus Wavelength for Pure Water and Sea Water 15
4. Relation Between Channel-4 and Channel-5 Signals Over Water (Linear Plot) 18
5. Relation Between Channel-4 and Channel-5 Bottom-Reflected Signals (Log-Log Plot) 18
6. MSS ERTS Data, Little Bahama Bank, 10 October 1972 21
7. Portion of H.O. 5990 Depth Chart 22
8. Ratio Depth Chart, Little Bahama Bank 24
9. Single-Channel Depth Chart, Little Bahama Bank 26
10. Aerial Photograph of Turbidity Plumes Formed by Action of Fish Schools 28
11. Aerial Photograph of Sand Bars, Little Bahama Bank 29
12. ERTS Frame 1169-15171-4 (Little Bahama Bank, 8 January 1973) 30
13. ERTS Frame 1277-15174-4 (Little Bahama Bank, 26 April 1973) 31
14. Portion of Lake Survey Chart 70, Northwest Lake Michigan 32
15. ERTS Frame 1089-16090 (Upper Lake Michigan, 20 October 1972) 34
16. Comparison Between Digital Depth Chart (Strip 1) Made by Optimum Decision-Boundary Method from ERTS Frame 1089-16090 and Lake Survey Chart 702 (Washington Island to Point Detour) 36
17. Comparison Between Digital Depth Chart (Strip 2) Made by Optimum Decision-Boundary Method from ERTS Frame 1089-16090 and Lake Survey Chart 702 (Moonlight Bay to Rawley Bay) 38

TABLES

1. Estimated U.S. Losses Through U.S. Commercial Ship Casualties 9
2. Number of Vessels Involved in U.S. Commercial Ship Casualties — Primary Causes 9
3. ERTS MSS Detector Characteristics 11
4. Input Parameters for Digital Processing of Bahama Bank Data 25
5. Channel-4 Signals Versus Depth 25
A-1. Input Variables for DEPTH1 Program 44
A-2. Listing of DEPTH1 Program 45
B-1. Input Variables for DEPTH2 Program 51
B-2. Listing of DEPTH2 Program 52

REMOTE BATHYMETRY AND SHOAL DETECTION WITH ERTS

1
INTRODUCTION

The successful launch and operation of ERTS-1 has provided a wealth of information in the form of multispectral imagery and data tapes covering all the continental U. S. and its coastal waters, as well as a large fraction of the shallow-water areas in the rest of the world. In these shallow-water areas, bottom features can frequently be seen on ERTS imagery to depths of nearly 10 meters in clear Caribbean waters and of 2-3 meters in more turbid northern waters. In view of the pressing need for updating hydrographic charts in coastal areas, the present study was initiated in an effort to extract quantitative water-depth information from ERTS data.

Aerial photography has long been used by the U. S. Coast and Geodetic Survey for the purpose of locating aids to navigation, mapping shorelines, and revealing bottom features to be investigated [1, 2]. The U. S. Naval Oceanographic Office also has used stereo-photogrammetric techniques for determining water depths in certain areas [3]. Numerical techniques for calculating water depth on the basis of the intensity of bottom-reflected solar radiation have been developed at ERIM and successfully applied to aircraft multispectral data [4]. These techniques now have been applied to ERTS data. In addition, new methods have been developed specifically for ERTS data.

In this report, these techniques are documented and the results of their application to two test sites discussed. The use of ERTS data for the purpose of remote bathymetry is then evaluated in terms of relative costs and accuracies, as compared with conventional ship-survey techniques. Finally, the results obtained from ERTS data are compared with those which might be obtained with space sensors that are more optimally designed for this application.

Two computer algorithms have been developed for extraction water-depth information from ERTS data. The ratio method (see Appendix A) corrects for differences in bottom reflectance and/or water attenuation and gives accurate results for depths up to the attenuation depth in ERTS Band 5 (about 3 meters in clear water). The optimum decision-boundary method (see Appendix B) extracts the maximum amount of depth information in the case of uniform bottom reflectance and water attenuation, but it is liable to errors when these parameters are not uniform throughout the scene.

Accuracy could be improved, and changes in bottom topography could be detected, by a time study of a sequence of ERTS frames for a given area. It is recommended that a computer method of comparing these frames be developed in conjunction with the MIDAS system currently being developed at ERIM.

In the meantime, processing of ERTS data should continue with presently developed techniques in areas where doubtful shoals exist or where erosion potential is high. Applications of these techniques could contribute interim data valuable to the shipping industry and establish baseline information for future erosion studies.

2
APPLICATIONS AREA DISCUSSION

2.1 UPDATING NAVIGATION CHARTS

The history of navigation and shipping is filled with examples of ship losses resulting from collisions with uncharted shoals or shoals whose positions were known only approximately. The International Hydrographic Office has expressed concern over the status of navigation charts around the world and has called upon the world community to assist in providing more reliable chart information.

One of the benefits that can be predicted from the use of satellites in mapping the oceans is improving nautical charts where better location and depth information of shoals would help reduce ship casualties. Additional benefits might be in helping to shorten commercial shipping routes and to increase safety. The reduction in commercial-ship casualties would reduce losses of life, cargo, and property. Table 1 [5] gives an estimate of the average losses for the U.S., which run over $90 million per year. Since U.S. shipping is about 10% of the total for commercial ships of 100 or more gross tonnage, about $1 billion is the estimated world-wide loss. The number of vessels involved and the primary cause of U.S. ship casualties are given in Table 2 [5]. At least one loss category is directly attributed to inaccurate depth information. In addition, it is possible that other loss categories might be indirectly reduced with better navigation charts, which could reduce calculated risks or shorten shipping routes. In any event, the reduction in loss on a world-wide basis is estimated at a few million dollars per year.

The use of ERTS remote bathymetry for this purpose has several advantages over conventional ship-survey techniques. First, the coverage is continuous, providing a two-dimensional image rather than a series of points or transects. This means that all shoals are much more likely to be detected, if they are within the range of the technique and their geographical locations can be easily determined by reference to land areas within the image. Second, ERTS coverage is repetitive, covering the same area every 18 days, so that changes resulting from coral growth and shifting sand bars can be assessed. Finally, because remote bathymetry is less expensive per unit area than conventional methods, areas which were previously uncharted because of economic constraints can now be charted.

TABLE 1. ESTIMATED U.S. LOSSES THROUGH U.S. COMMERCIAL SHIP CASUALTIES (IN DOLLARS)

Kind of Loss	1966	1967	1968	1969	1970	1971
Vessel	95,139,000	53,080,000	63,206,000	68,267,000	69,274,000	78,961,000
Cargo	7,454,000	9,801,000	5,186,000	10,269,000	17,360,000	6,629,000
Property	3,131,000	12,262,000	12,676,000	7,926,000	10,629,000	8,911,000

This table has been constructed using fiscal-year figures published in the following issues of the Proceedings of the Marine Safety Council: December 1966; November 1968; December 1969; December 1970; and December 1971.

TABLE 2. NUMBER OF VESSELS INVOLVED IN U. S. COMMERCIAL SHIP CASUALTIES—PRIMARY CAUSES

Primary Cause	1966	1967	1968	1969	1970	1971
Personnel Fault	550	551	984	1,193	1,300	1,325
Calculated Risk*	257	386	307	124	22	10
Restricted Maneuvering Room	210	177	50	32	31	22
Storms-Adverse Weather	374	202	446	253	274	370
Unusual Currents	50	34	70	46	57	19
Sheer, Suction, Bank Cushion	36	31	34	57	3	4
Depth of Water Less than Expected	100	63	110	76	54	50
Failure of Equipment	311	376	540	610	510	524
Unseaworthy-Lack of Maintenance	340	323	135	133	86	81
Floating Debris-Submerged Object	153	157	97	151	172	151
Inadequate Tug Assistance	137	105	34	63	30	14
Fault on Part of Other Vessel or Person	746	947	1,142	1,333	1,304	1,435
Unknown-Insufficient Information	29	23	62	112	220	147
TOTAL	3,293	3,030	4,001	4,183	4,063	4,152

The source of the figures is the same as for Table 1.

*Before 1969, "Error in Judgment-Calculated Risk," rather than just "Calculated Risk."

In order to take best advantage of the greater range and accuracy of conventional techniques, the two methods should be used in conjunction; satellite bathymetry can be used to detect and locate shoals, and conventional ship surveys to confirm their depths at sampled points and chart surrounding areas to greater depths.

2.2 MONITORING SHORELINE CHANGES

The bottom topography of coastal areas is constantly changing as a result of the natural processes of erosion and deposition. These processes are accelerated by storms and changing water levels in inland lakes. They are also modified, either intentionally or unintentionally, by the construction of harbors, recreational beaches, power-generation plants, marinas, and local erosion-abatement devices.

There is need for a rapid monitoring technique to measure changes in coastal topography over wide areas. Such a capability could be used to assess storm damages, identify areas of high erosion risk, and evaluate the impact of shoreline construction. Information gathered by this process could be used, for example, by the Environmental Protection Agency for zoning purposes or by the U.S. Army Corps of Engineers for building more effective erosion-control devices.

Because of its repetitive wide-area coverage and low cost, ERTS obviously has potential for this type of application. Aircraft multispectral data and conventional depth-sounding techniques could be used in conjunction with ERTS data to obtain greater accuracy and resolution. The techniques of remote bathymetry are documented in the following chapter, and the potential of ERTS data for this application is evaluated in the remainder of this report.

3
EXTRACTION OF WATER-DEPTH INFORMATION FROM ERTS MSS DATA

3.1 GENERAL CONSIDERATIONS

The ERTS multispectral scanner receives electromagnetic radiation in the four spectral bands indicated in Table 3. The radiance at the detector is measured and converted into an integer data value V_i between 0 and 63. In the linear mode the signal is directly proportional to the radiance at the detector. That is,

$$V_i = k_i R_i \tag{1}$$

where R_i is the radiance in band i at the detector, and k_i is the sensitivity constant for the detector (see Table 3). In the signal-compression mode of ERTS, the signal is not linearly proportional to the radiance (see Figure 1) but the relationship may be considered approximately linear over the middle range of signal values.

TABLE 3. ERTS MSS-DETECTOR CHARACTERISTICS [6]

Band	Wavelength Range (μm)	Maximum Radiance (mw cm^{-2} sr^{-1})	Sensitivity Constant (mw^{-1} cm^2 sr)
4	0.5-0.6	2.48	25.4
5	0.6-0.7	2.00	31.5
6	0.7-0.8	1.76	35.8
7	0.8-1.1	4.60	13.7

The radiance observed over shallow water is the result of sunlight reflecting from the bottom and the water surface, as well as of the scattering of sunlight in the water and the atmosphere. That part of the signal resulting from bottom reflection contains information about the depth of the water through which the light has passed. In order to extract this information, one must first separate the bottom-reflection signal from the rest of the observed signal, and then determine how this signal is related to the water depth.

Assuming the linear relationship (see Eq. 1) is correct, the signal observed over shallow water may be expressed as follows:

$$V_i = k_i R_{pi} + k_i \tau_i R_{si} + k_i \tau_i \frac{H_i}{\pi} \rho_i \frac{1}{n^2} e^{-\alpha_i (\sec \theta + \sec \phi) z} \tag{2}$$

where R_{pi} = atmospheric path radiance
τ_i = atmospheric transmittance
R_{si} = radiance resulting from (water) surface reflection
H_i = solar irradiance incident on water surface
ρ_i = bottom reflectance
n = index of refraction of water
α_i = attenuation coefficient of water
θ = angle of observation (under water)
ϕ = solar-zenith angle (under water)
z = water depth

This equation neglects volume scattering of sunlight from the water itself, which is usually small compared to the other components when conditions are favorable (i.e., when the water is fairly clear).

The first term of this equation accounts for the scattering of sunlight by the atmosphere; the second for the specular reflection of diffuse sky radiation by the water surface. The reflection of direct sunlight from the water surface into the scanner, known as sun glint, is avoided by restricting angles of observation to less than the solar-zenith angle (see Figure 2).

Since these two terms contain no information about the water depth, they are considered as the background signal which must be removed before the actual depth processing is done. This background signal,

$$V_{bi} = k_i R_{pi} + K_i \tau_i R_{si} \tag{3}$$

may be determined by scanning over deep water, where there is no bottom-reflected signal. When this background signal is subtracted from the data, the remainder represents the light

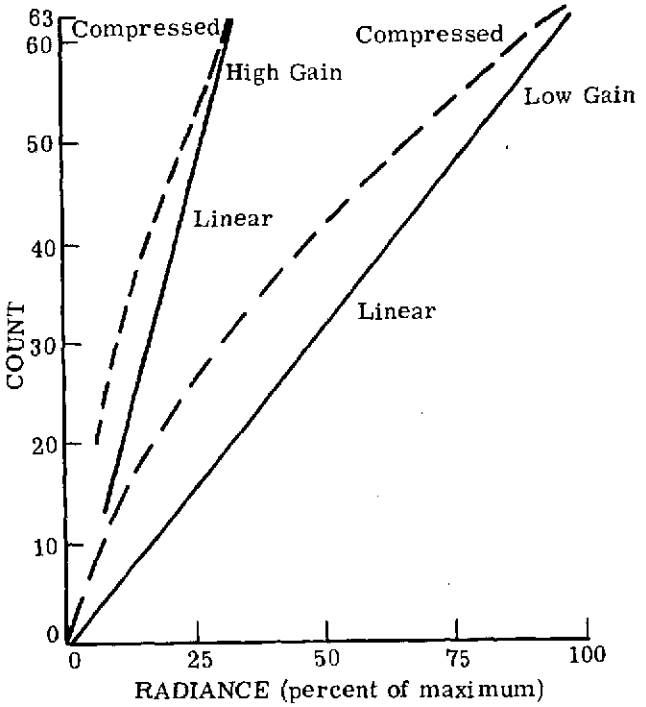

FIGURE 1. MSS OUTPUT COUNT (V_i) VERSUS RADIANCE (R_i/R_{max}), COMPRESSED AND LINEAR MODES

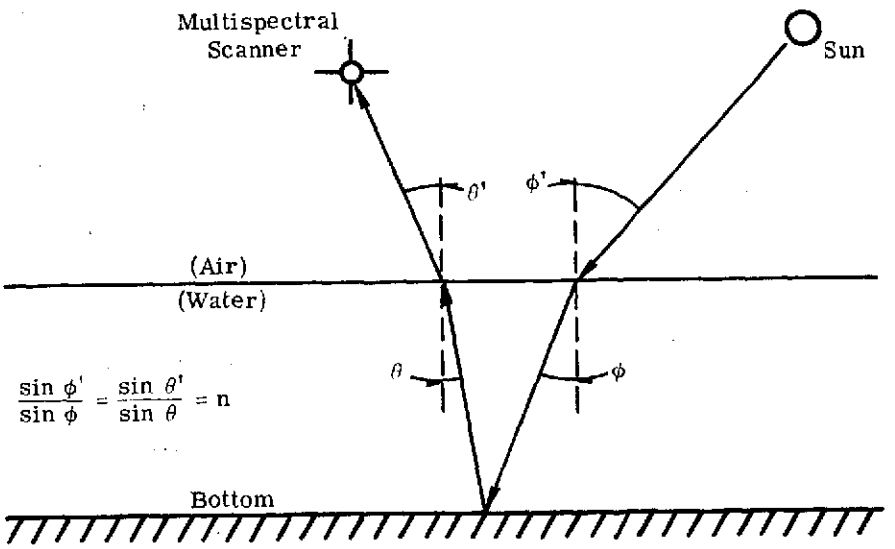

FIGURE 2. GEOMETRY OF WATER-DEPTH MEASUREMENT

which has been reflected from the bottom and attenuated in the intervening water layer. From Equation (2), this part of the signal may be expressed as

$$\Delta V_i = V_i - V_{bi} = k_i \tau_i \frac{H_i}{\pi} \rho_i \frac{1}{n^2} e^{-\alpha_i (\sec \theta + \sec \phi) z} \tag{4}$$

The depth dependence of this signal arises from the attenuation of light in the water, expressed by the exponential factor in this equation. Methods of calculating the water depth at each point in the scene are discussed in the following four sections.

3.2 SINGLE-CHANNEL METHOD

If all the parameters in Equation (4) are known, it may be inverted to yield the water depth, as follows

$$z = \frac{1}{\alpha_i (\sec \theta + \sec \phi)} \ell n \left(\frac{\Delta V_{oi}}{\Delta V_i} \right) \tag{5}$$

where

$$\Delta V_{oi} = k_i \tau_i \frac{H_i}{\pi} \rho_i \frac{1}{n^2} \tag{6}$$

This latter quantity, which is interpreted as the bottom-reflected signal at zero water depth, may be determined either from Equation (6) or from examining the scanner signal at the water's edge.

The attenuation coefficient α_i may be estimated from Figure 3, although there is a wide variation in the attenuation coefficients depending on the purity of the water. Alternately, if the water depth is known at one point in the scene, the attenuation coefficients may be deduced from Equation (5). They may also be measured in the laboratory, of course, if samples of the water are taken from the scene.

With ERTS data, the scan angle θ is small enough so that sec θ may be approximated by 1. There is then a unique signal level associated with each water depth, assuming that the water-attenuation coefficient and bottom reflectance remain constant throughout the scene. A water-depth chart may then be produced simply by mapping the most penetrating channel (i.e., the channel with the smallest attenuation—channel 4 for ERTS). In such a map, a distinct symbol is printed out at each point in the scene for each range of data values specified. By using Equation (5), we can specify these ranges to correspond to convenient depth ranges.

The advantage of this method is its simplicity and relative insensitivity to random noise in the data. It has two drawbacks, however. First, from an operational standpoint, it is

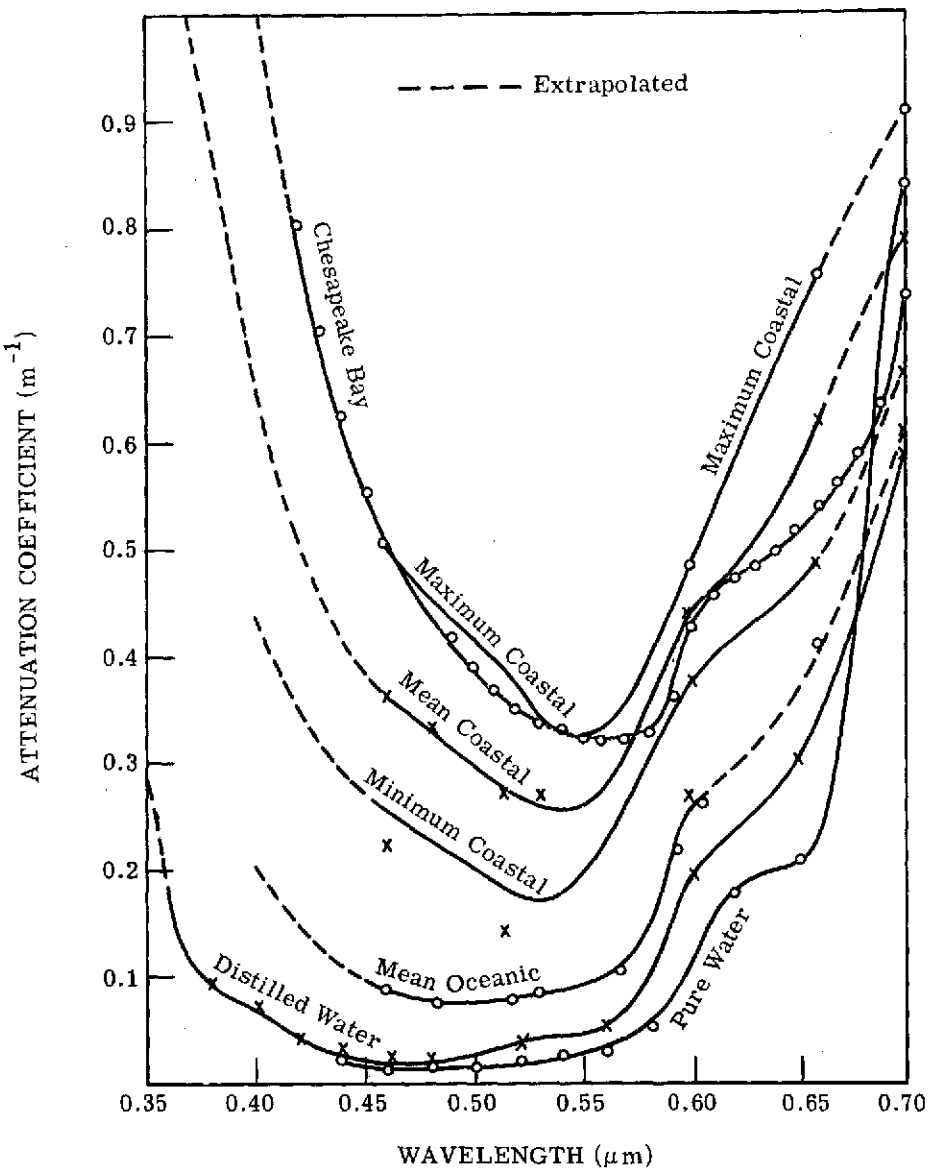

FIGURE 3. ATTENUATION COEFFICIENT VERSUS WAVELENGTH FOR PURE WATER AND SEA WATER [7]

difficult to accurately estimate the water-attenuation coefficient without some ground-truth data: either the depth must be known at one point in the scene, or a sample of water must be collected and analyzed in the laboratory. Second, if there are variations in either the water attenuation or the bottom reflectance within the scene, systematic errors will be introduced into the calculated depth. Both of these drawbacks are eliminated or reduced—but at the cost of greatly increased sensitivity to random noise—in the ratio method discussed in the following section.

3.3 RATIO METHOD

If one takes the ratio of the bottom-reflected signals in two spectral bands i and j, Equation (4) yields:

$$\frac{\Delta V_i}{\Delta V_j} = \frac{k_i \tau_i H_i \rho_i}{k_j \tau_j H_j \rho_j} e^{-(\alpha_i - \alpha_j)(\sec\theta + \sec\phi)z} \tag{7}$$

This equation may be inverted to give the following equation for water depth:

$$z = \frac{1}{(\alpha_j - \alpha_i)(\sec\theta + \sec\phi)} \ln\left(\frac{\Delta V_i}{\Delta V_j} R_{ji}\right) \tag{8}$$

where

$$R_{ji} = \frac{k_j \tau_j H_j \rho_j}{k_i \tau_i H_i \rho_i} \tag{9}$$

This method of calculating water depth from two channels has several advantages over the single-channel method. As mentioned in the previous section, the attenuation coefficients and bottom reflectances change from one location to another, from one time to another at the same location, and even from one point to another within the same scene. However, the difference between the attenuation coefficients in two appropriately chosen bands exhibits much less variation from point to point and from time to time (see Figure 3). The same is true of the ratio of the bottom reflectances in the two channels. Since only this difference and this ratio appear in Equation (8), the results using this method are much less sensitive to changes in water quality and bottom type than are the results of the single-channel method. This means that (1) it is easier to specify input parameters for this method, and that (2) there are fewer systematic errors inherent in the results.

The ratio method of extracting water depths from multispectral data appears to be a powerful and useful technique. However, it does require optimum channel selection and a high signal-to-noise ratio in the data. ERTS bands 4 and 5 are useful for water-depth work but not optimum. In addition, the low gain setting reduces the usefulness of channel 5 for determining maximum water depths. Even under the best conditions, the bottom-returned signal in channel 5

falls below the noise level for depths greater than a few meters. The non-linear response characteristics of ERTS in the compressed mode also cause problems in the application of this method to ERTS data.

In processing the Bahama Bank data, a two-step procedure was used to extend the range of the depth chart. First, the ratio method was applied, using minimum coastal values for the water-attenuation coefficients (from Figure 3). This resulted in a chart with a maximum depth of about 2.8 meters. These depths were then visually correlated with the channel-4 data values, and this correlation was then used to determine the actual attenuation coefficient for channel 4. By this procedure we determined that the water actually falls in the mean oceanic category (the ratio-depth results are still valid for this case because the difference between the channel-4 and channel-5 attenuation coefficients is the same for both types of water). This attenuation coefficient was then used to produce a single-channel depth chart, with a maximum depth of about 9 meters.

3.4 OPTIMUM DECISION-BOUNDARY METHOD

In processing the Lake Michigan-Green Bay Inlet data, the ratio method was found to be restrictive because of the poor quality of the data. The combination of low sun elevation (30^{o}) and relatively high water attenuation restricted the penetration depth to about 2 meters in channel 4 and less than 1 meter in channel 5. The number of points for which depth could be calculated by the ratio method was too small to apply the two-step procedure used for the Bahama Bank data. Consequently, the data were examined more thoroughly, and a third method was developed for extracting water depth from this type of noisy data.

Equation (4) predicts a correlation between the data values observed over water in channels i and j, of the form

$$\log (\Delta V_i) = \frac{\alpha_i}{\alpha_j} \log (\Delta V_j) + \log k \tag{10}$$

where k is a constant depending on bottom reflectance, scene illumination, etc. Points selected from the Lake Michigan test site are plotted in Figures 4 and 5. The log-log plot (Figure 5) shows a linear correlation between ΔV_1 and ΔV_2, with a regression coefficient:

$$\frac{\alpha_2}{\alpha_1} = 1.5 \tag{11}$$

The ratio of the attenuation coefficients in the two channels can be obtained by this method. Therefore, if the difference in the attenuation coefficients can be estimated from Figure 3, their absolute values can also be determined without ground-truth data.

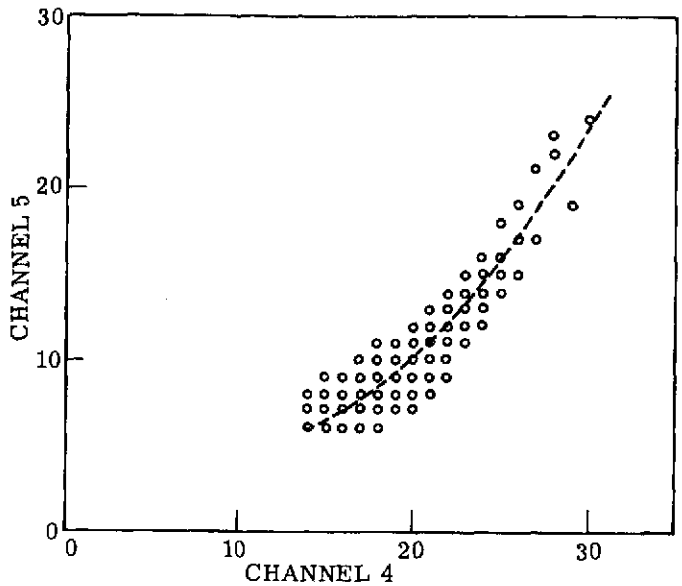

FIGURE 4. RELATION BETWEEN CHANNEL-1 AND CHANNEL-2 SIGNALS OVER WATER (LINEAR PLOT)

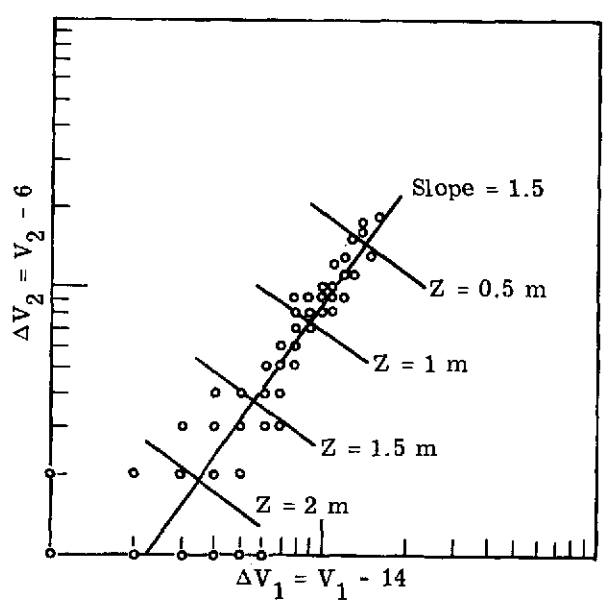

FIGURE 5. RELATION BETWEEN CHANNEL-4 AND CHANNEL-5 BOTTOM-REFLECTED SIGNALS (LOG-LOG PLOT)

Figure 5 also suggests a method for estimating depth which is less sensitive to noise than the single-channel method. In the single-channel method, the decision boundaries for depth are vertical lines in Figure 5. However, assuming the actual data points are randomly distributed around the orthogonal regression line in Figure 5, the optimum-decision boundaries for classifying these points are lines drawn perpendicular to this curve. Thus, if a given data point falls between the lines marked z = 1 m and z = 1.5 m, the water depth at this point should be classified in this range. This procedure is mathematically implemented by the following equation:

$$z = \frac{1}{c}\sum_{i=1}^{N} \alpha_i \log\left(\frac{\Delta V_{oi}}{\Delta V_i}\right) \tag{12}$$

where

$$c = (\sec\theta + \sec\phi)\sum_{i=1}^{N} \alpha_i^2 \tag{13}$$

and ΔV_{oi} is defined by Equation (6).

This method may be applied to any number of channels (N). The main advantage is an improvement over the single-channel method in the accuracy of classification. Variations in water attenuation and bottom reflectance may cause systematic errors, as in the single-channel method, but they can perhaps be minimized by a judicious choice of channels. These errors also can be reduced by means of the time-study method described in the following section.

Equation (12) was implemented in a computer program (see Appendix B) and applied to the Lake Michigan test site, using ERTS bands 4 and 5. No attempt has yet been made to find the optimum channels for this method, since only two penetrating channels are available on ERTS. Results of this application are discussed in Section 4.

3.5 ERROR REDUCTION BY TIME-STUDY TECHNIQUES

Errors introduced by variations in water quality, clouds, and other transient phenomena can be reduced by a repeated analysis of the same scene over a period of time, using any of the three methods described above. Averaging the results on a point-by-point basis should reinforce the stable features, as well as reduce the transient effects.

A photographic overlay method would probably be the most feasible way of carrying out this averaging process at present. While the capability of averaging two scenes on a point-by-point basis by computer is not yet available, it should be possible in the near future with the

MIDAS hybrid computer system now under development at ERIM. The repetitive coverage afforded by ERTS also should qualify ERTS data for this type of treatment.

4
DISCUSSION OF RESULTS

4.1 LITTLE BAHAMA BANK

The primary test site for this study had been designated as an area west of Puerto Rico where several doubtful shoals are reported on the Hydrographic Office charts. However, this area was obscured by clouds during the first ERTS passes, and no useful data were obtained. Consequently, processing was started on an alternate test site north of Grand Bahama Island, covered by ERTS frame 1079-15165 (see Figure 6).

These data were obtained on 10 October 1972 at 16:15 GMT, when the solar elevation was 47.4^{o}. The principal point of the image is at 27.45^{o} N, 78.82^{o} W (northwest of Grand Bahama Island). The frame covers approximately 100×100 nautical miles, with Grand Bahama Island in the lower right-hand corner and the Little Bahama Bank covering most of the lower half of the frame. There is a 30% cloud cover, but most of the clouds are in the upper half of the frame, over deep water. There is a small patch of clouds in the center of the Bank and over Grand Bahama Island.

MSS band 4 (0.5 to 0.6 μm) shows many underwater features north of Grand Bahama Island. Most of these can be identified on the Hydrographic Office depth chart (see Figure 7), but a number of streaks radiate from the center of the Bank which are not on the chart. The significance of these streaks is discussed below.

MSS band 5 (0.6 to 0.7 μm) shows some underwater features, but the penetration depth of this channel is clearly less than that of MSS band 4.

MSS band 6 (0.7 to 0.8 μm) and 7 (0.8 to 1.1 μm) show no underwater features, but they are useful for defining the land-water interfaces.

Digital processing of this data began with our applying the ratio method described in Section 3.3 to MSS bands 4 and 5. The computer program implementing this method is listed and described in Appendix A. The input parameters for this program were obtained from the Smithsonian Physical Tables, except for the background or deep-water signals which were obtained from the scanner data itself. These values are shown in Table 4.

The maximum depth which can be computed by this method is the depth at which the channel-5 signal falls below the noise level. For this data set, using only the best of the six

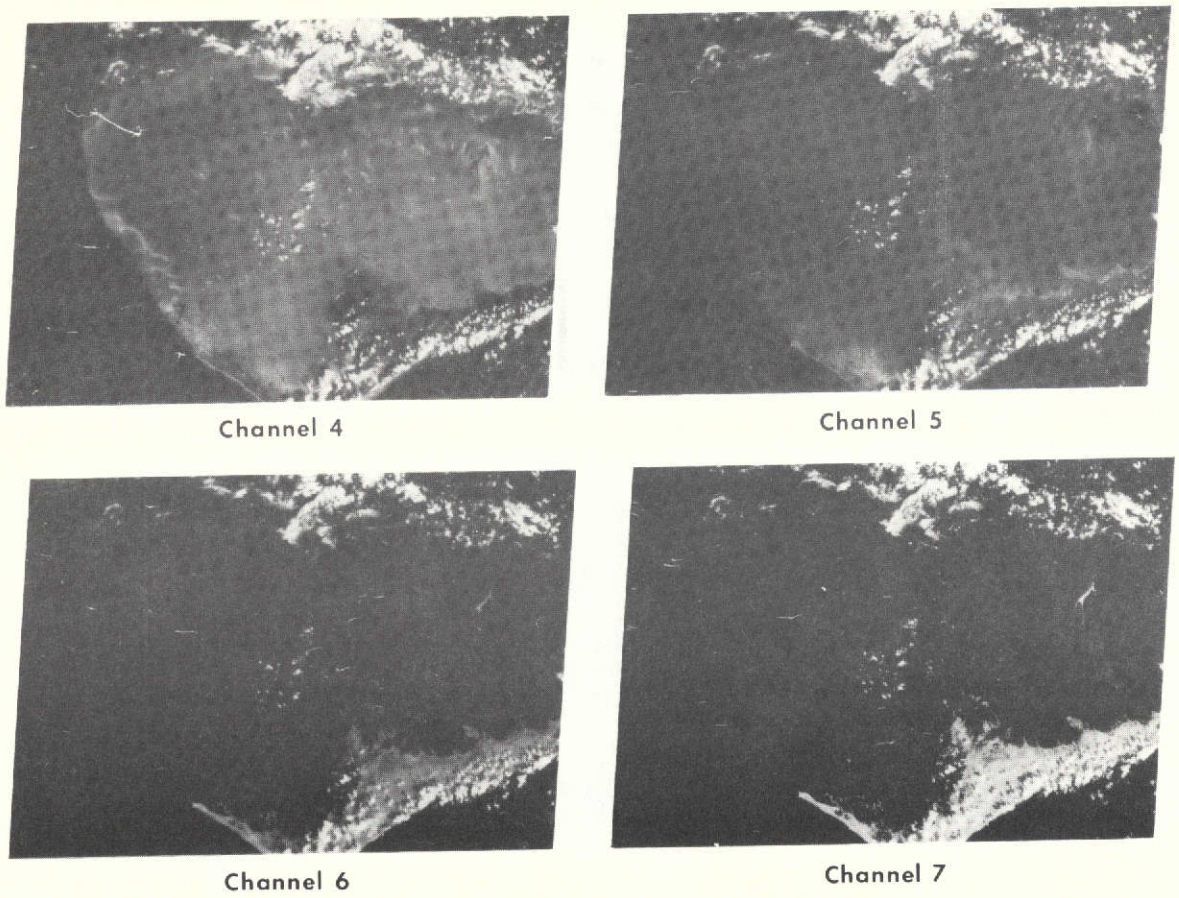

FIGURE 6. MSS ERTS DATA, LITTLE BAHAMA BANK, 10 OCTOBER 1972

FIGURE 7. PORTION OF H.O. 5990 DEPTH CHART

ERTS detectors, this maximum depth is about 2.8 meters. The depth chart produced by this method is shown in Figure 8.

In order to extend the depth range of this chart, a second map was made using only channel 4, which penetrates to a much greater depth than channel 5. To calibrate this single-channel map, the channel-4 data values were correlated with the depths obtained from the ratio method. From this correlation, an attenuation coefficient of 0.10 m^{-1} was inferred for channel 4. This is in agreement with published values for mean oceanic conditions (see Fig. 3). Using this attenuation coefficient, we extrapolated the relationship between the channel-4 signal and the water depth to a depth of 9 meters. This relationship is shown in Table 5, and the depth chart based upon this relationship is shown in Figure 9.

There are a few discrepancies between the depths indicated on these two maps, notably in the area around Memory Rock (on the western edge of the Bank) where the ratio method gives greater depth values than the single-channel method, and around Cormorant Point (on the center of Grand Bahama Island) where the reverse is true. These discrepancies probably are due to the presence of different bottom materials in these areas. The area around Memory Rock appears bright on the MSS-4 imagery and dark on the MSS-5 imagery, indicating that the bottom material is probably a bright green coral. The area around Cormorant Point is dark on both the MSS-4 and MSS-5 imagery, perhaps the result of dark organic material washed from the land. In both cases the ratio method gives more accurate depths, as expected.

The single-channel map (Figure 9) shows two other anomalies (see Fig. 9b). First there are erroneous depth values near the clouds in the center and at the upper edge of the scene. These are due to cloud shadows and scattering from the clouds themselves. Second, there are numerous streaks apparently radiating outward from the center of the Island, where the depth is indicated between 1 and 2 meters. These could be either sediment plumes formed by schools of fish, or shifting sand bars. Aerial photographs of both these phenomena (Figures 10 and 11) confirm the former hypothesis. ERTS frames taken on 8 January 1973 (Figure 12) and 26 April 1973 (Figure 13) show streaks of varying length and direction similar to those in Figure 10 but in different locations thus supporting their association with the action of fish schools in search of food.

4.2 LAKE MICHIGAN

The second data set processed during the course of this study was ERTS frame 1089-16090, which covers the northwestern corner of Lake Michigan, including the inlet to Green Bay where there are numerous shoals and small islands, and the east coast of the Door Peninsula where there are several shallow bays (see Figure 14). The date of this ERTS pass was 20 October 1972. The solar elevation was 30° during the pass, resulting in a scene illumination almost 50 percent lower than in the Bahama Bank scene.

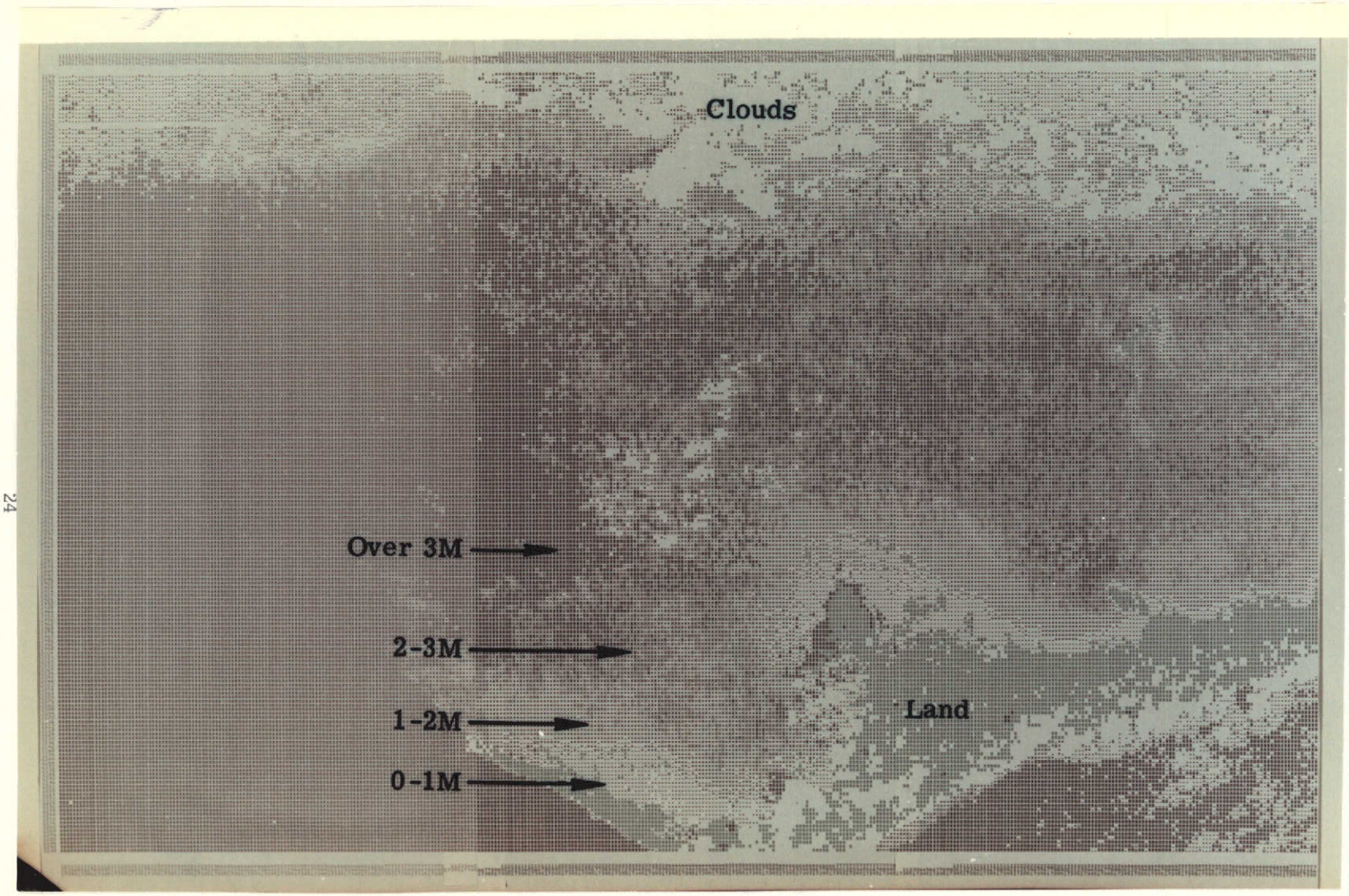

FIGURE 8. RATIO DEPTH CHART, LITTLE BAHAMA BANK
Original figure in color.

TABLE 4. INPUT PARAMETERS FOR DIGITAL PROCESSING OF BAHAMA BANK DATA

Input Parameter	Value
$\alpha_2 - \alpha_1$	0.26 m^{-1}
ρ_2/ρ_1	1.26
H_2/H_1	0.92
τ_2/τ_1	1.07
V_{b_1}	22 counts
V_{b_2}	11 counts
ϕ	42.6°

TABLE 5. CHANNEL-4 SIGNALS VERSUS DEPTH

Channel-4 Signals (counts)	Depth (m)	Chart Symbols (Fig. 9)
20-24	9 - ∞	M (blue)
25-26	7 - 9	X (blue)
27-29	5 - 7	* (blue)
30-33	3 - 5	· (blue)
34-36	2 - 3	= (red)
37-40	1 - 2	X (red)
41-45	0 - 1	M (red)

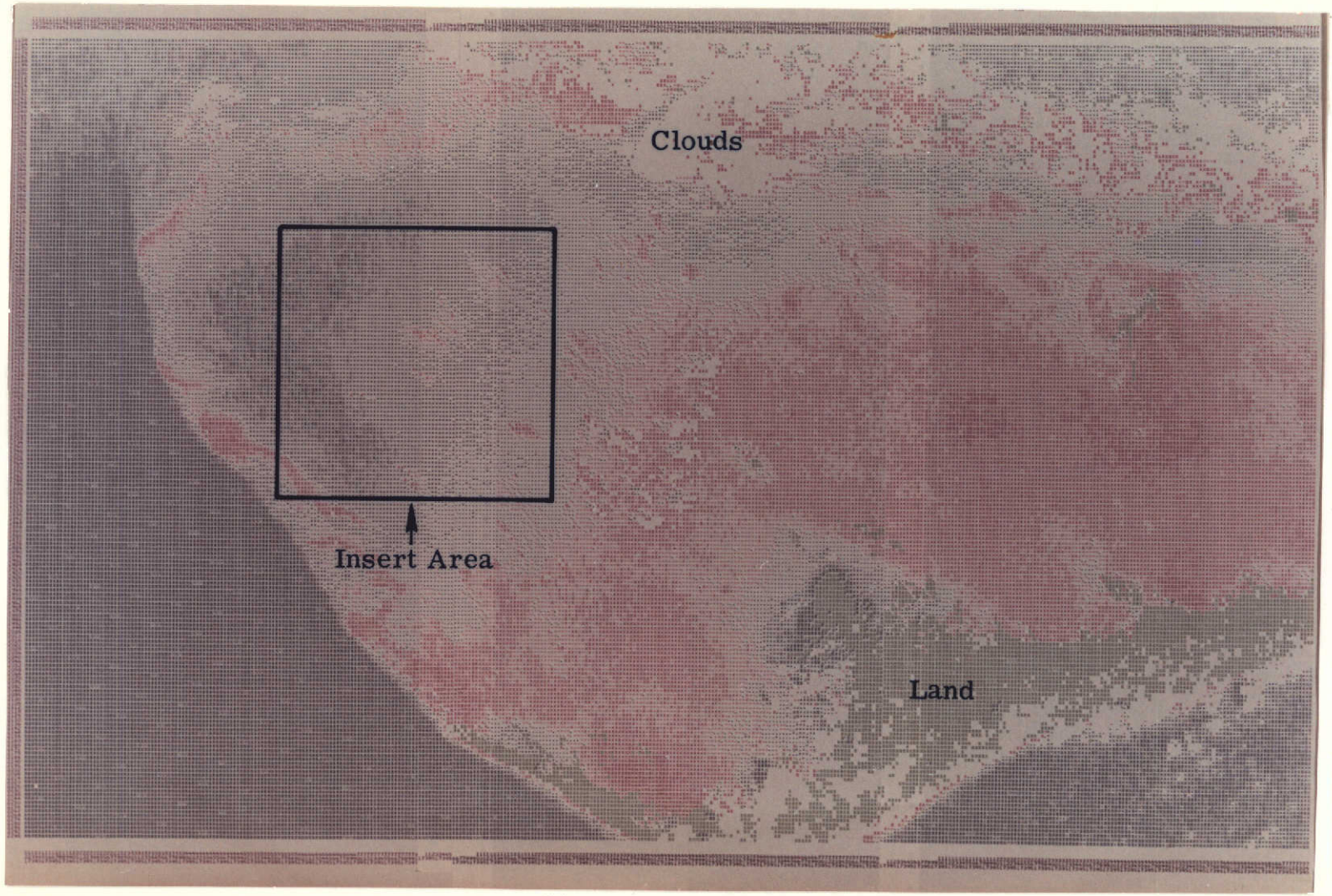

(a) Large-Area Map

FIGURE 9. SINGLE-CHANNEL DEPTH CHART, LITTLE BAHAMA BANK
Original figure in color.

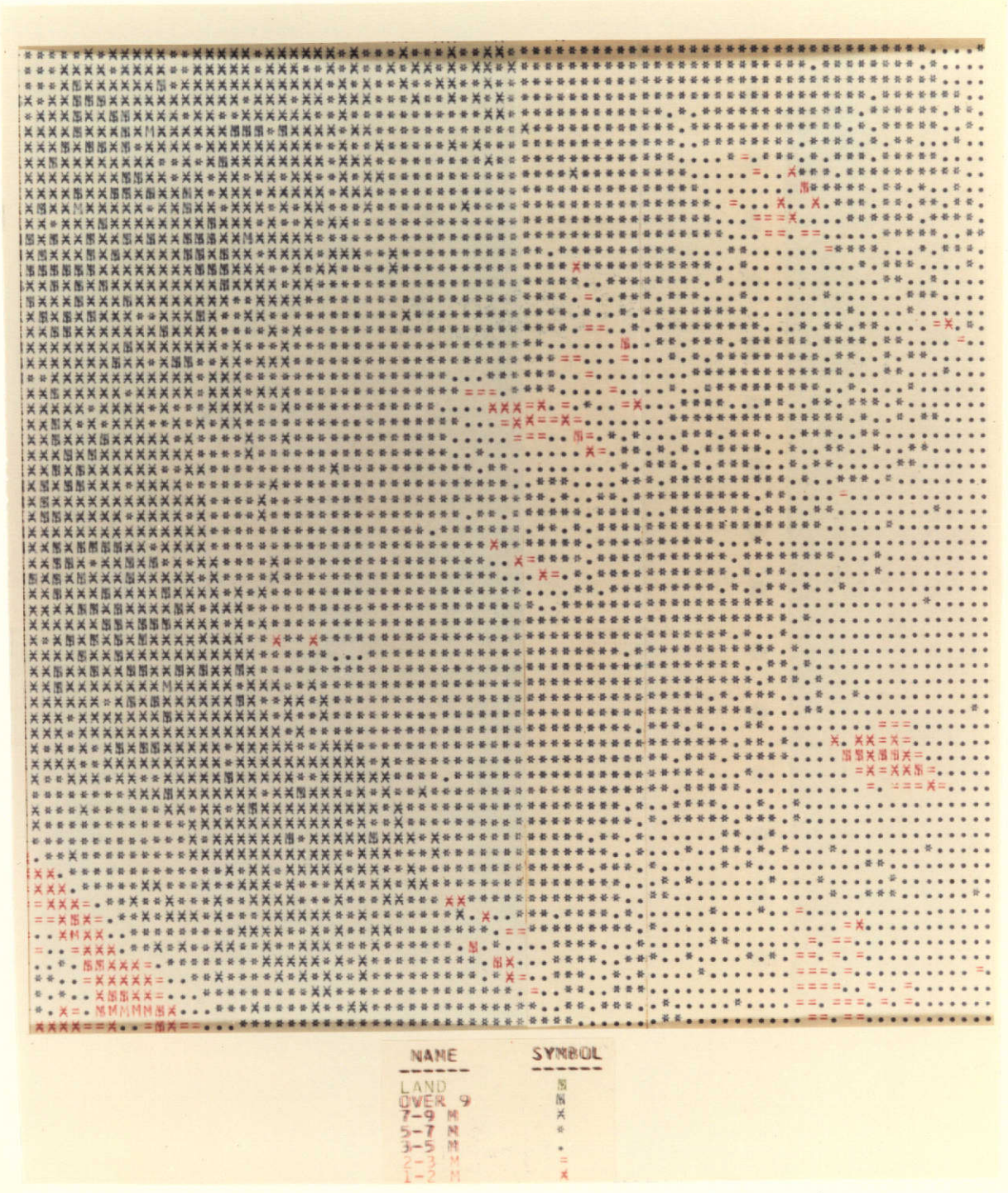

(b) Insert, showing Anomalies in Depth Values

FIGURE 9. SINGLE-CHANNEL DEPTH CHART, LITTLE BAHAMA BANK

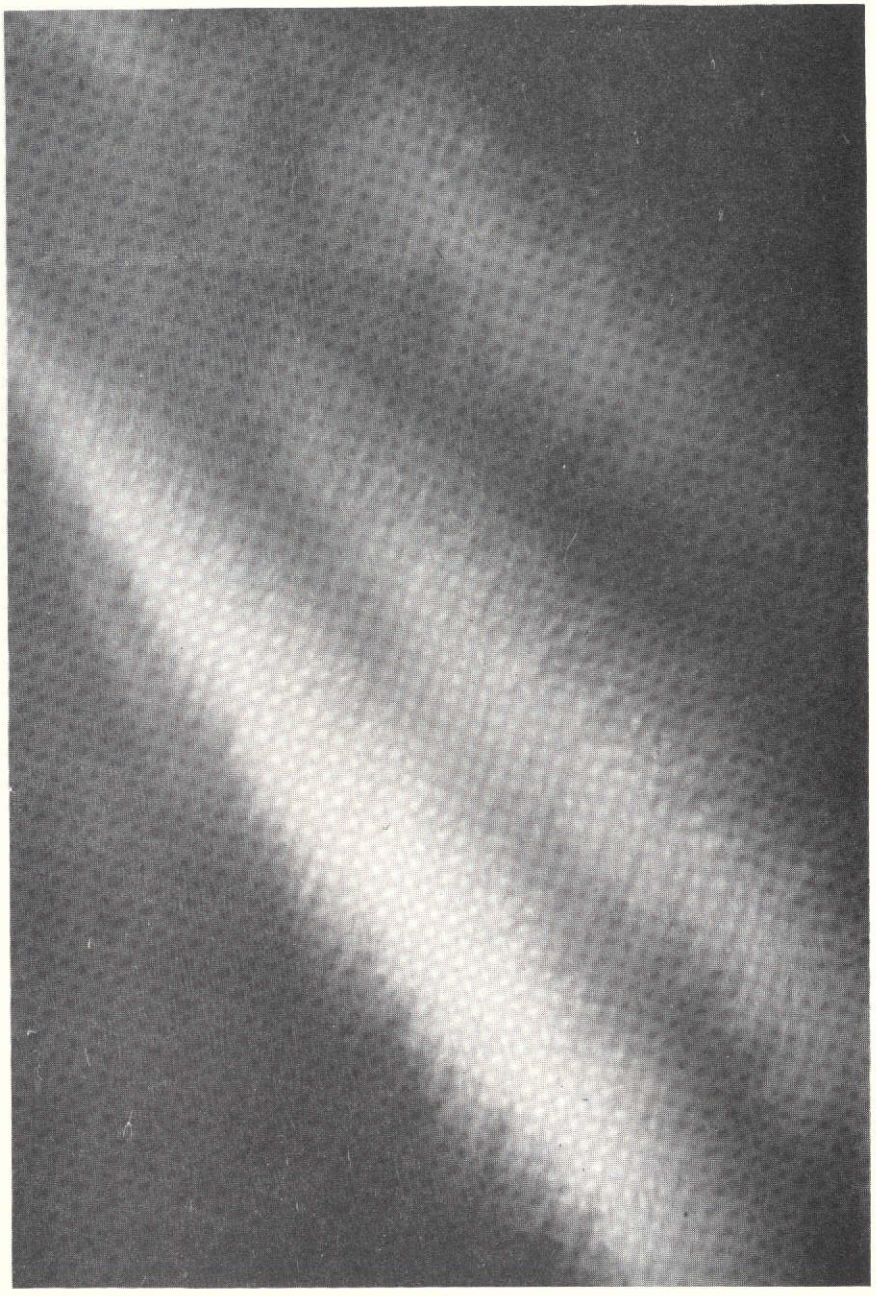

FIGURE 10. AERIAL PHOTOGRAPH OF TURBIDITY PLUMES FORMED BY ACTION OF FISH SCHOOLS. Little Bahama Bank, November 1973.

FIGURE 11. AERIAL PHOTOGRAPH OF SAND BARS, LITTLE BAHAMA BANK.
November 1973.

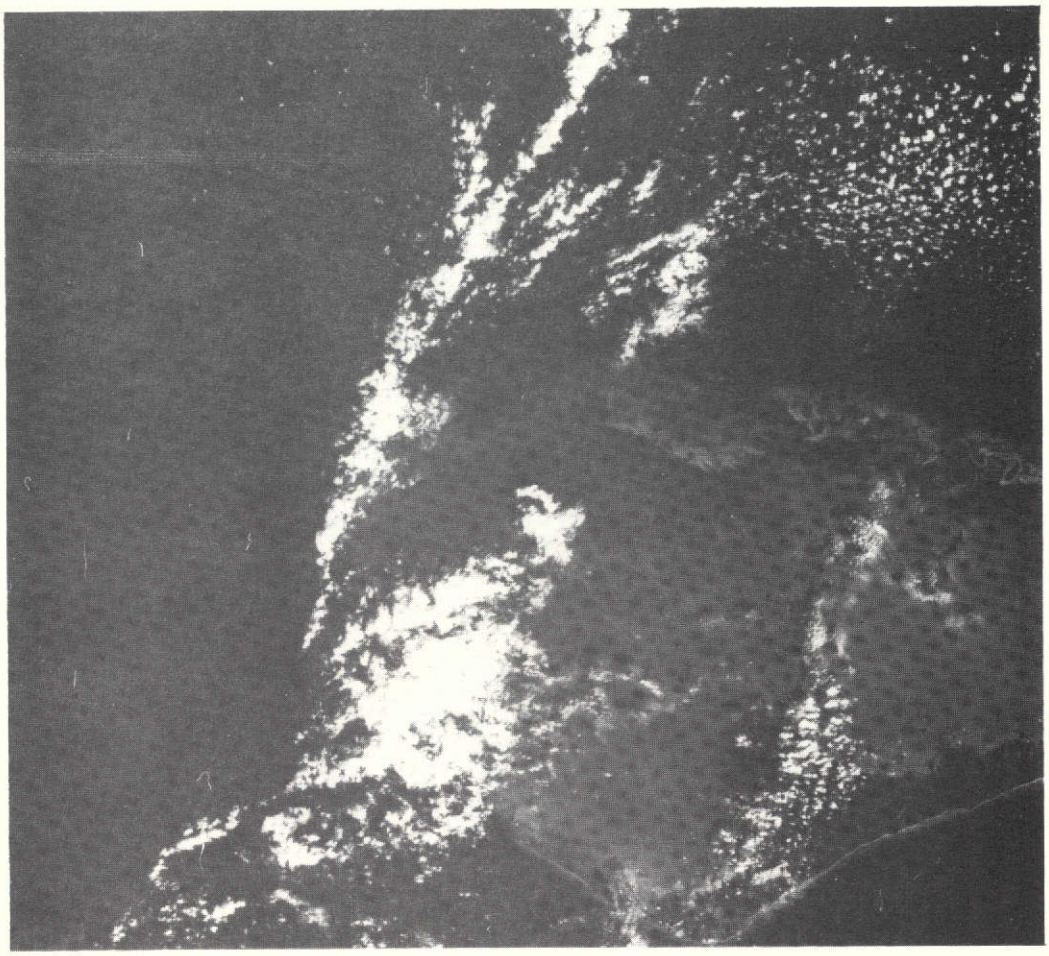

FIGURE 12. ERTS FRAME 1169-15171-4 (LITTLE BAHAMA BANK, 8 JANUARY 1973)

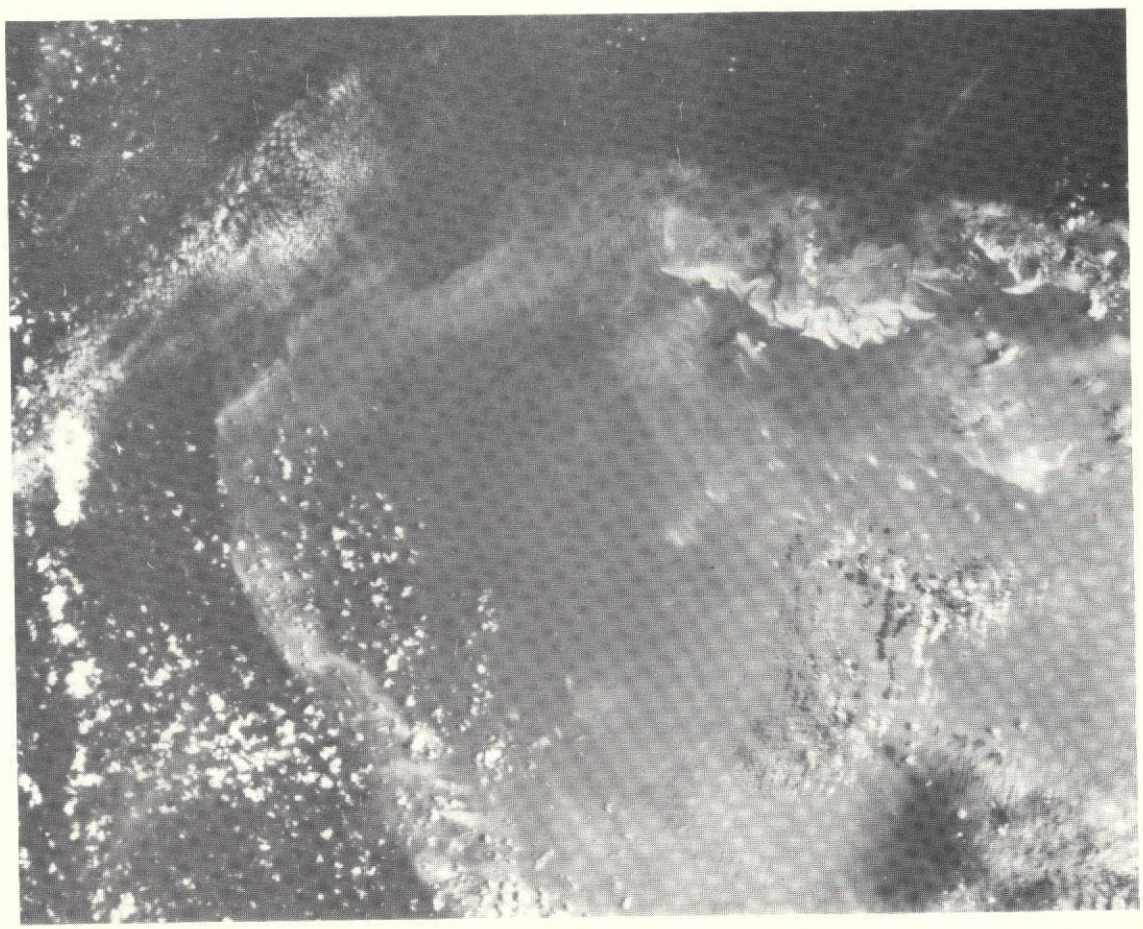

FIGURE 13. ERTS FRAME 1277-15174-4 (LITTLE BAHAMA BANK, 26 APRIL 1973)

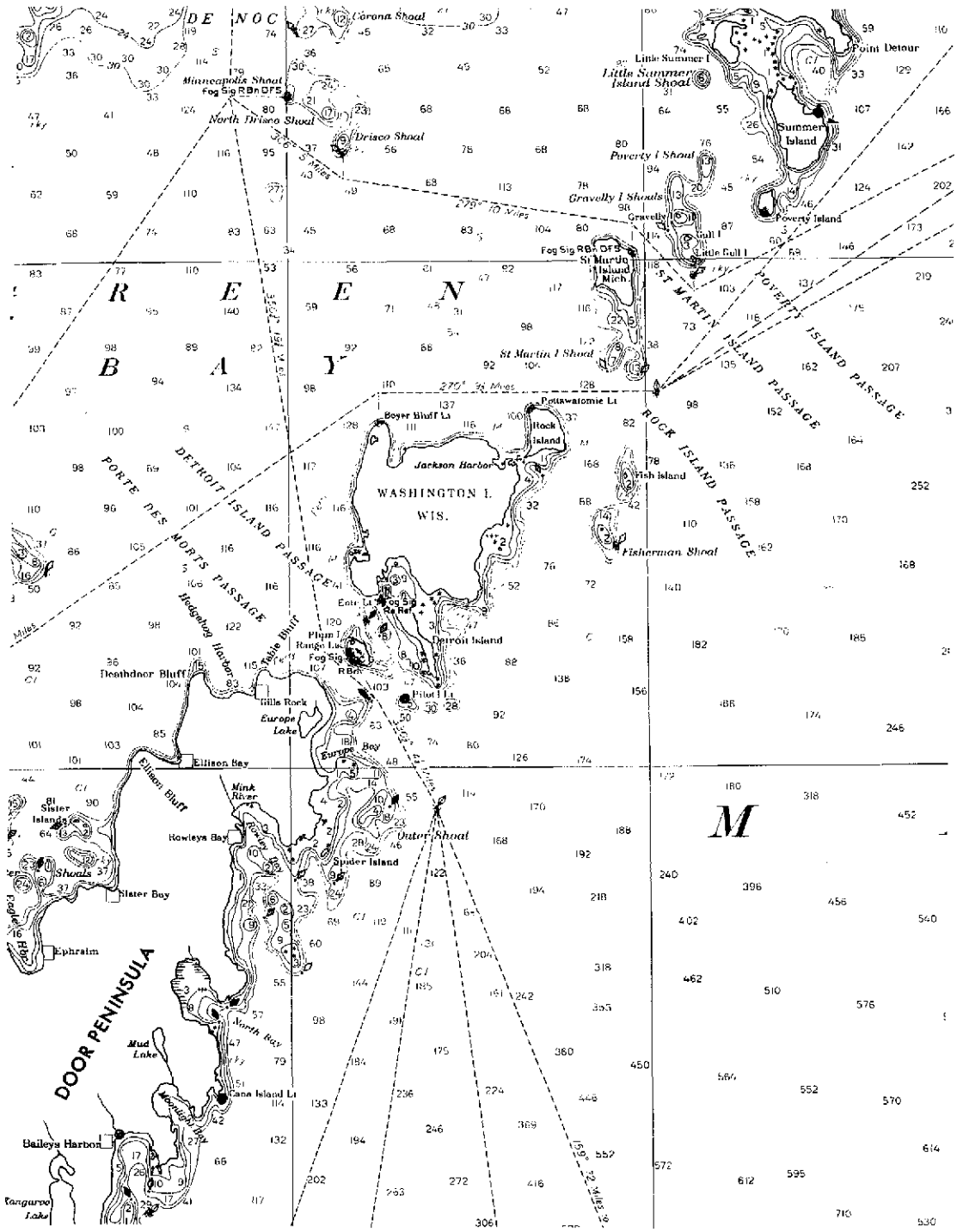

FIGURE 14. PORTION OF LAKE SURVEY CHART 70, NORTHWEST LAKE MICHIGAN

Some underwater features are visible on the MSS band-4 imagery along the Door Peninsula and the inlet to Green Bay (Figure 15). Very few underwater features are visible in band 5. The water seems to be fairly uniform, but much more turbid than the Bahama-Bank water.

Because of this combination of low sun angle and high water attenuation, the ratio-processing method did not produce any useful results. In an effort to improve upon the single-channel method, we examined the data and developed a third processing technique. This method makes use of optimum-decision boundaries for depth classification, as described in Section 3.4. From the correlation of channel-4 and channel-5 signals (see Figure 5) and published water-attenuation curves (see Figure 3), the water-attenuation coefficients were taken to be

$$\alpha_1 = 0.30 \text{ m}^{-1}$$
$$\alpha_2 = 0.45 \text{ m}^{-1} \qquad (14)$$

Using the combination of channel-4 and channel-5 signals indicated in Equation (12), the minimum signal that can be distinguished from the background noise corresponds to a depth of about 2 meters.

Two depth maps were produced by this method. The first map (Figure 16) covers most of the Green Bay inlet, from Point Detour to the Porte Des Morts Passage. The accuracy of this map was checked by comparison with Lake Survey Chart 702. Most of the features in the lower half of this region are accurately shown in the digital map, but some errors are present in the upper half as a result of increased turbidity in the water coming from Big Bay De Noc. Fisherman Shoal, east of Washington Island, is clearly shown on the ERTS map, and the water depths around Washington Island agree quite well with the Lake Survey Chart. St. Martin's Island Shoals (south of St. Martin Island) are beyond the depth range of the map, as is Poverty Island Shoal (northwest of Poverty Island). Little Summer Island Shoal should be just on the edge of detectability, but it is not indicated on the map. A number of false depth values appear in the 1.5-2.0 meter range as a result of turbidity to the north of St. Martin Island.

The second map (Figure 17) covers the eastern coast of the Door Peninsula from Bailey's Harbor to the end of the Peninsula. The depths indicated on this map are in good agreement with Lake Survey Chart 702. Rowley Bay, North Bay, and Moonlight Bay are accurately mapped, and Four Foot Shoal is detectable in the mouth of Rowley Bay. Nine Foot Shoal (near the tip of the Peninsula) is beyond the range of detectability and is not shown on the map.

The depth range of these maps should be at least doubled by using ERTS data with higher sun elevation. Data tapes and imagery have been received from ERTS passes over Lake Michigan during the summer of 1973 which show bottom features to a depth of 4-5 meters. Over a period of a few years, repeated ERTS coverage of the Great Lakes should yield data of sufficient quality to update navigation charts over large areas.

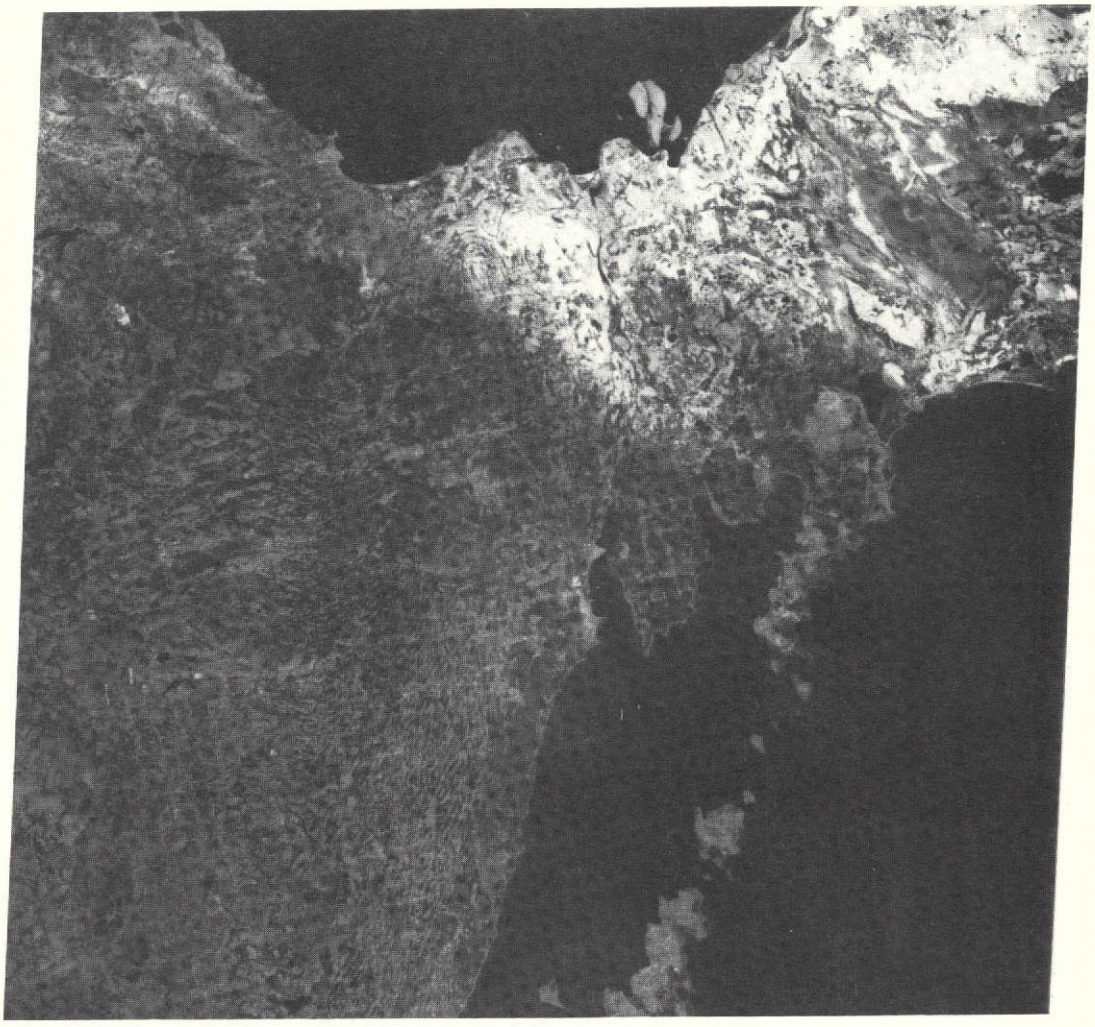

(a) Band 4

FIGURE 15. ERTS FRAME 1089-16090 (UPPER LAKE MICHIGAN, 20 OCTOBER 1972)

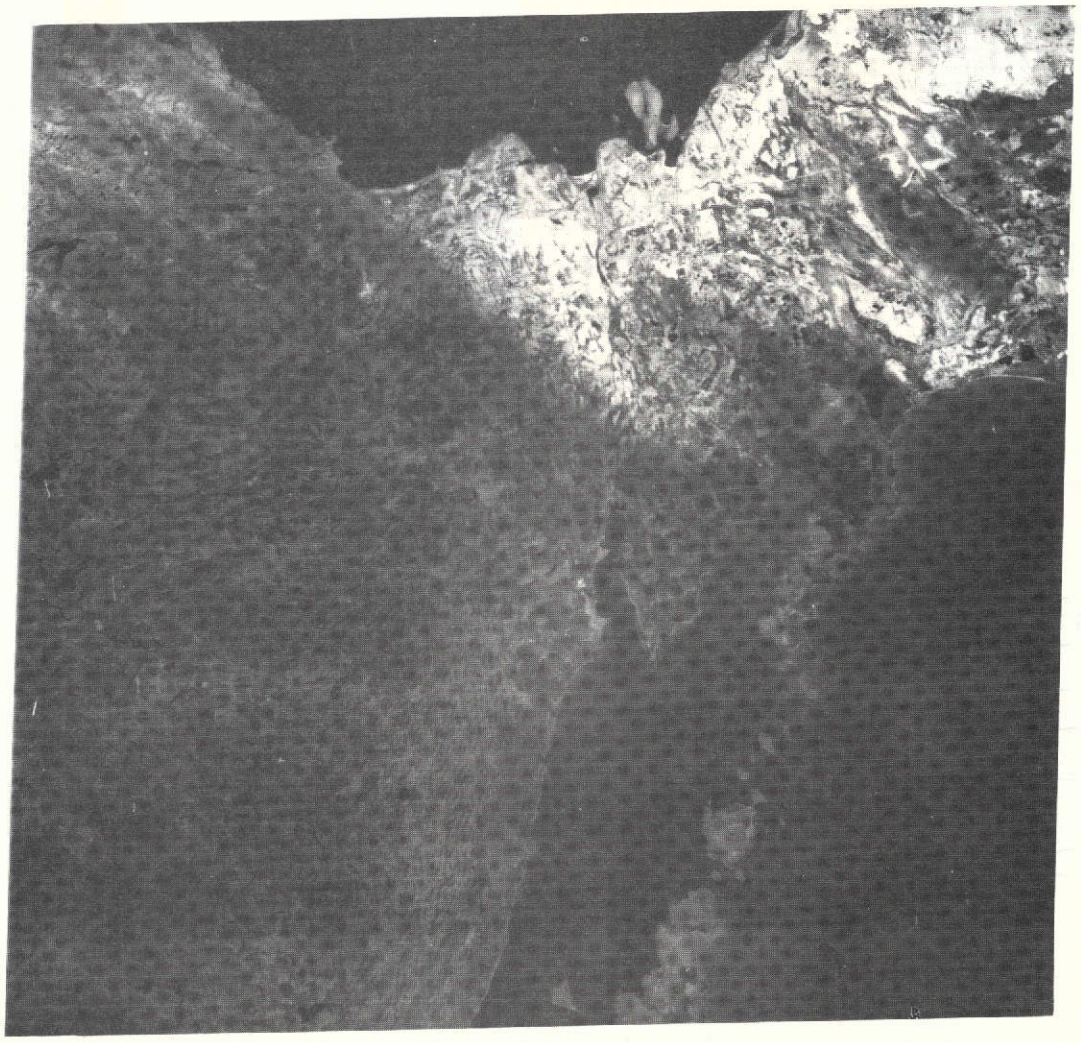

(b) Band 5

FIGURE 15. ERTS FRAME 1089-16090 (UPPER LAKE MICHIGAN, 20 OCTOBER 1972) (Concluded)

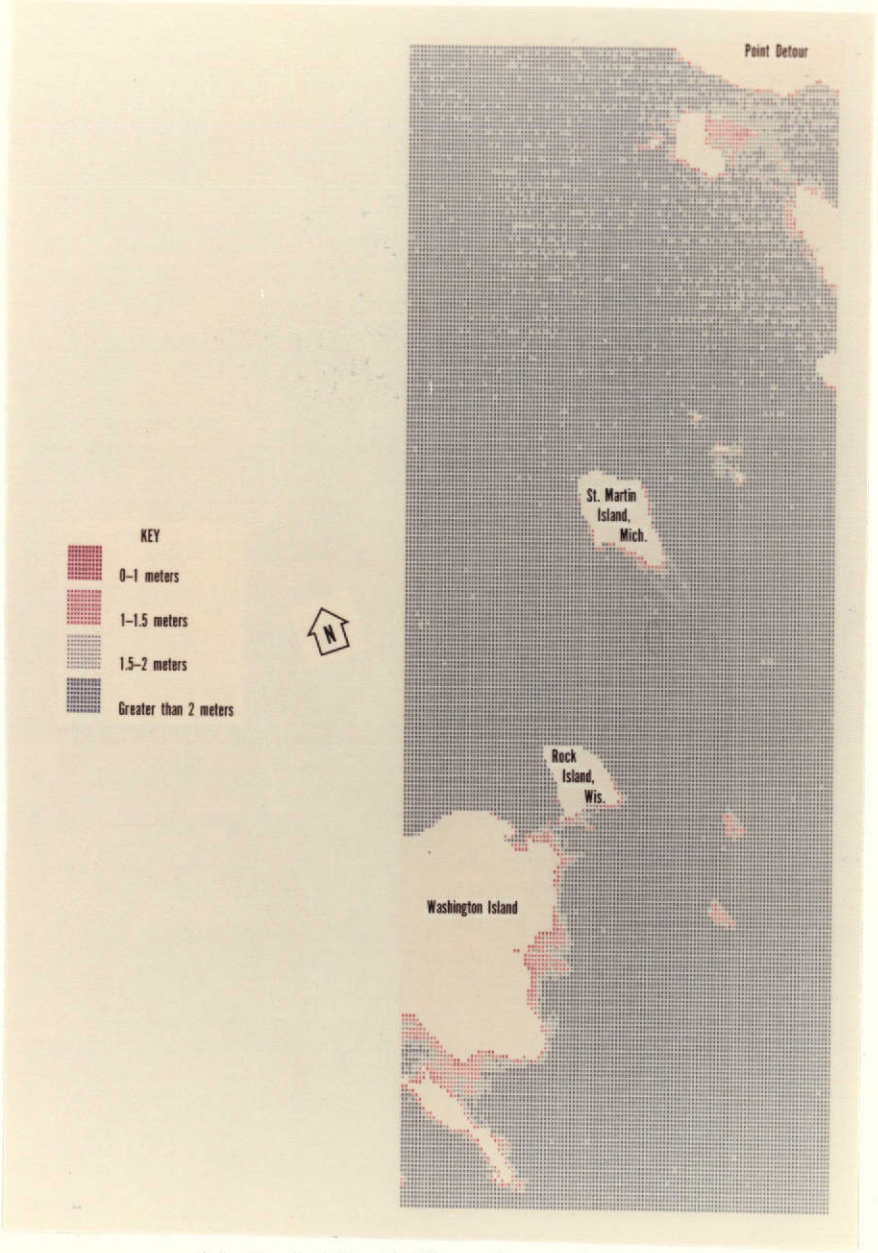

(a) Digital Depth Chart (Strip 1)

FIGURE 16. COMPARISON BETWEEN DIGITAL DEPTH CHART (STRIP 1) MADE BY OPTIMUM DECISION-BOUNDARY METHOD FROM ERTS FRAME 1089-16090 AND LAKE SURVEY CHART 702 (WASHINGTON ISLAND TO POINT DETOUR). The density of computer symbols denotes depth. Original figure in color. (Continued)

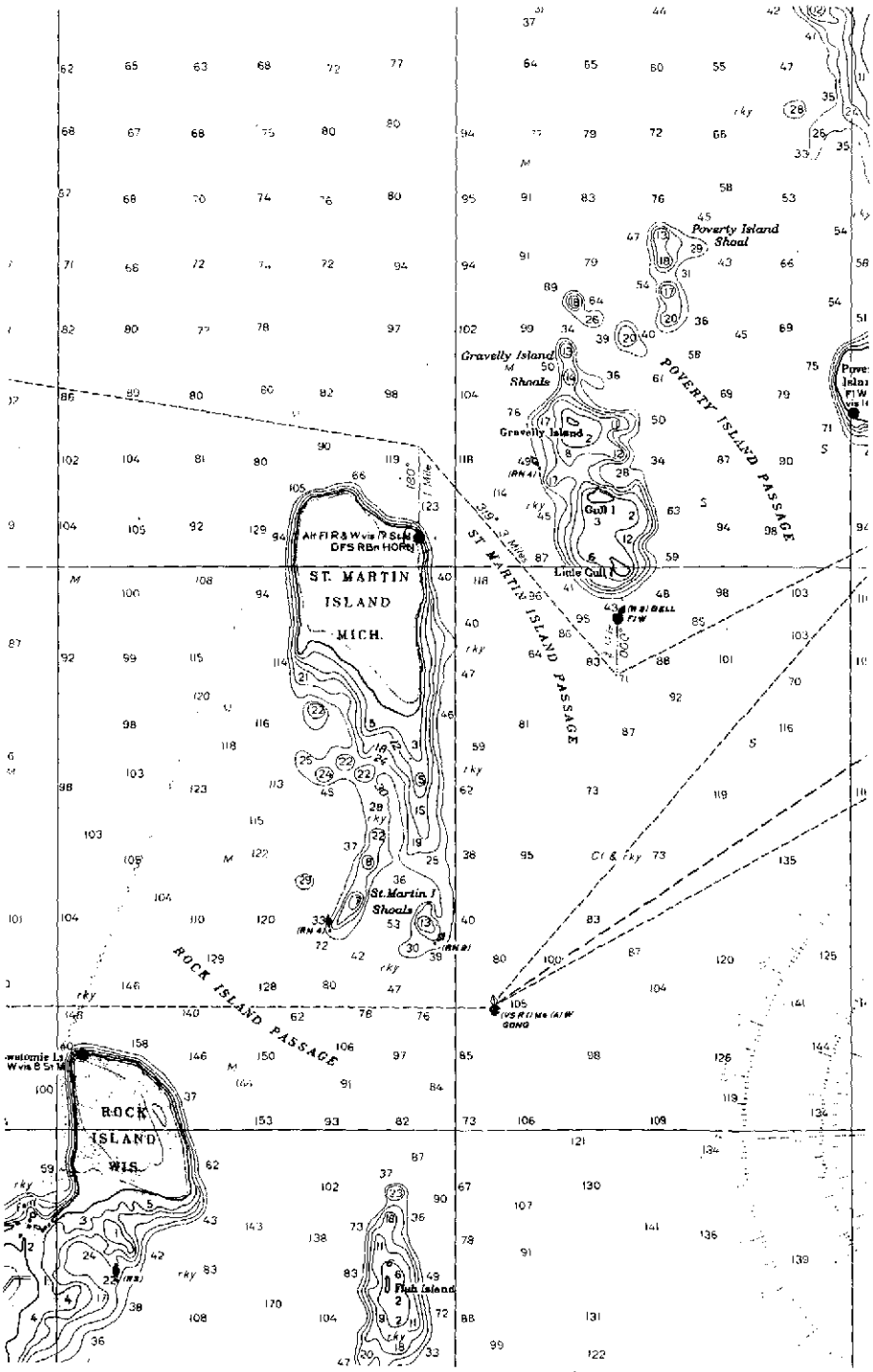

(b) Portion of Lake Survey Chart 702 (Washington Island to Point Detour)

FIGURE 16. COMPARISON BETWEEN DIGITAL DEPTH CHART (STRIP 1) MADE BY OPTIMUM DECISION-BOUNDARY METHOD FROM ERTS FRAME 1089-16090 AND LAKE SURVEY CHART 702 (WASHINGTON ISLAND TO POINT DETOUR) (Concluded)

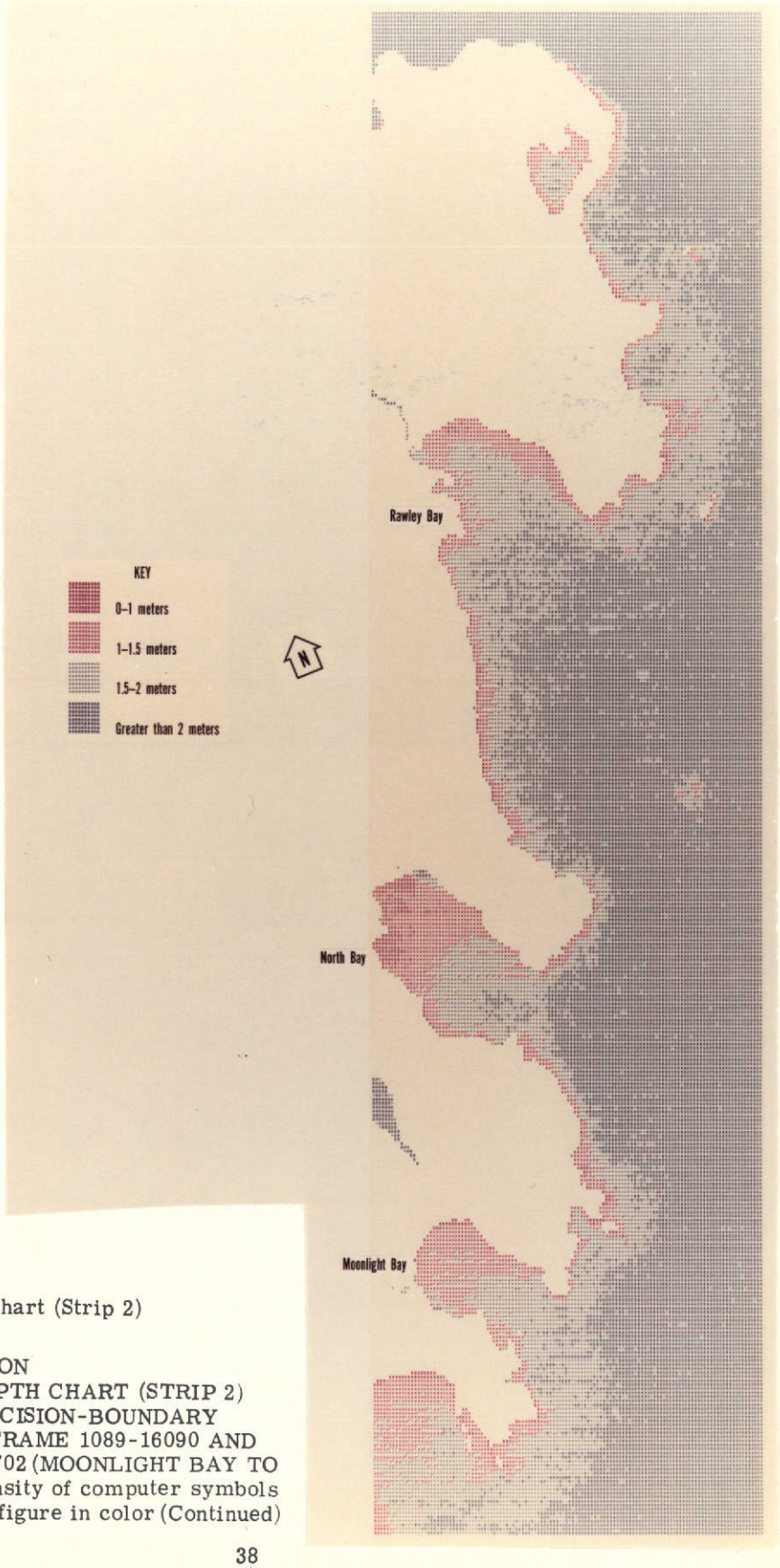

(a) Digital Depth Chart (Strip 2)

FIGURE 17. COMPARISON BETWEEN DIGITAL DEPTH CHART (STRIP 2) MADE BY OPTIMUM DECISION-BOUNDARY METHOD FROM ERTS FRAME 1089-16090 AND LAKE SURVEY CHART 702 (MOONLIGHT BAY TO ROWLEY BAY). The density of computer symbols denotes depth. Original figure in color (Continued)

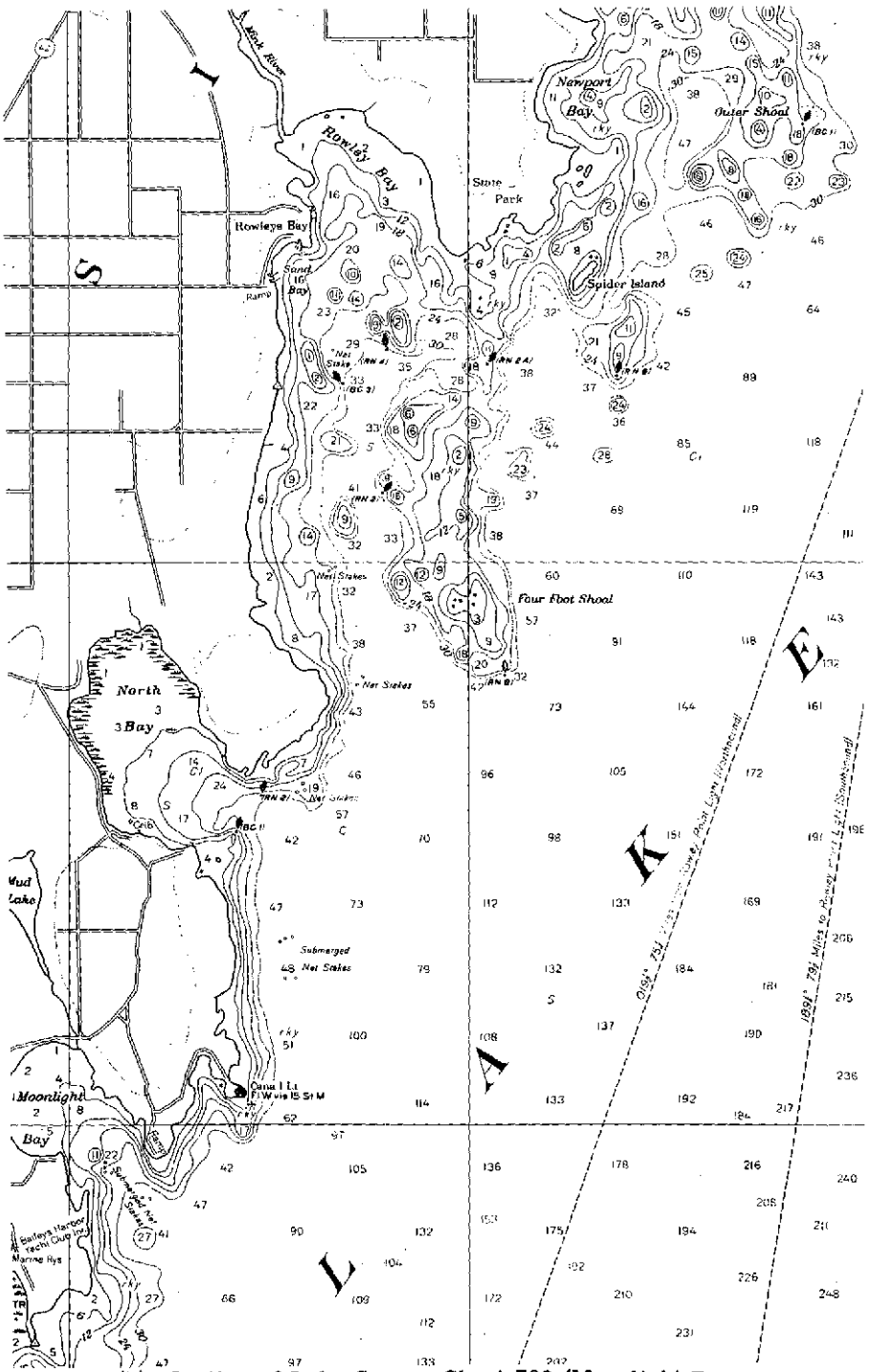

(b) Portion of Lake Survey Chart 702 (Moonlight Bay to Rowley Bay)

FIGURE 17. COMPARISON BETWEEN DIGITAL DEPTH CHART (STRIP 2) MADE BY OPTIMUM DECISION-BOUNDARY METHOD FROM ERTS FRAME 1089-16090 AND LAKE SURVEY CHART 702 (MOONLIGHT BAY TO ROWLEY BAY) (Concluded)

5
EVALUATION OF ERTS POTENTIAL FOR REMOTE BATHYMETRY

5.1 RELATIVE COSTS AND ACCURACIES OF REMOTE SENSING VERSUS SHIP SURVEYS

Costs for processing ERTS data to produce depth charts have been estimated to be on the order of $1.50 per square mile. Total costs for collecting and processing multispectral data are difficult to estimate, but they are probably at least an order of magnitude smaller than those involved in conventional ship-survey techniques. Accuracies of remote-sensing techniques are on the order of 10-20 percent for depths at which multispectral techniques can be used to correct for differences in bottom reflectance and water attenuation (i.e., where bottom-reflected signals are observed in at least two channels).

The accuracy of modern ship-survey techniques is on the order of 2-3 percent. Some charts, however, contain data based on survey records from the early 19th century, when the available techniques probably yielded less accurate results than present-day, remote-sensing techniques. The time and equipment required for conventional ship surveys have prevented many countries from updating these charts. Even the maps distributed by U. S. agencies contain many doubtful shoals indicated by "position approximate" and "existence doubtful."

ERTS data is presently available, and is still being collected, for areas in which conventional ship-survey techniques are too slow and too costly to adequately update hydrographic charts or to keep up with changing conditions. In these areas, the use of remote bathymetric techniques in conjunction with ERTS data could make a valuable contribution to the store of hydrographic information now available.

5.2 EVALUATION OF ERTS VERSUS BETTER SPACE SENSORS FOR MEASURING WATER DEPTH

The utility of ERTS data for bathymetric purposes is limited by the gain and band location of the ERTS sensor. With the low gain setting normally used, an approximate dynamic range of only 20 counts can be observed in the bottom-reflected signal under optimum conditions. The water-depth range corresponding to this signal range is approximately equal to the attenuation length $1/\alpha$. This depth range could be increased by almost 50 percent by increasing the gain by a factor of 4 and encoding the data to 8 bits instead of 6.

For clear Caribbean water, the attenuation length is about 10 meters in ERTS band 4 and about 3 meters in band 5. These could be increased by narrowing the bands and positioning them closer to the wavelength of minimum water attenuation (c.f., Figure 3).

An example of a better space sensor for measuring water depth is the Skylab S-192 multispectral scanner.

Band 3 (0.50-0.55 μm) of this sensor has half the bandwidth of ERTS band 4, and it is positioned very near to the point of minimum water attenuation. The attenuation length of Caribbean water in this channel is about 12.5 meters. This, combined with the 8-bit precision of Skylab data, allows depths of 15 meters to be seen on Skylab scanner data.

The repetitive coverage of ERTS is a positive feature which might be explored further, using the time-study techniques described in Section 3.5.

These could be used to reduce errors and study changes in bottom topography over a period of time.

In summary, although ERTS is not an optimum sensor for this application, there is a large amount of depth information in ERTS data which could be extracted by the techniques documented in this report. The value of this information would seem to justify further processing of ERTS data by these techniques, as well as developing new techniques for comparing a time sequence of ERTS frames of a given area.

Appendix A
COMPUTER PROGRAM FOR RATIO METHOD

A computer program implementing the ratio method discussed in Section 3.3 was written during the course of this contract. This program performs the functions of subtracting the background signal (see Equation 3) and computing the depth from a specified pair of channels (see Equation 8). This computation is done at each point in the scene, and the results are written on an output tape. The program also can compute the depth simultaneously from several different pairs of channels. The result of the computation for each pair of channels is written out as a separate channel on the output tape, followed by the mean and standard deviation of the values calculated from each pair of channels.

The input variables for this program are summarized in Table A-1. These are specified in the flexible READ AND PRINT DATA format in MAD language. The actual computer coding, in MAD language, is listed in Table A-2.

TABLE A-1. VARIABLES FOR DEPTH1 PROGRAM

	Input Variables	Mode	Description
Card 1:			
	NV	Integer	No. of channels on input tape
	NC	Integer	No. of channels on output tape (NC=NPAIRS + 2)
Card 2:			
	Process Variables		
	INBIN	Integer	Bin no. of input tape
	OUTBIN	Integer	Bin no. of output tape
	UNIT	Integer	Unit on which input tape is mounted
	OUNIT	Integer	Unit on which output tape is mounted
	NSA	Integer	Array containing line and point numbers of scene
Card 3:			
	Input Variables		
	COEFSW	Integer	If COEFSW=0, a coefficient tape containing the deep-water (surface-reflection) signal at each point number must be put in If COEFSW=1, a single value for the deep-water signal is read in for each channel (see below)
	DEEP (I)	Integer	The deep-water signal in channel I (I=1 . . . NV)
	NPAIRS	Integer	No. of pairs of channels used
	PAIRS (I)	Integer	Channel numbers used (I=1 . . . 2*NPAIRS)
	ALPHA (I)	Floating Point	Water attenuation coefficient in channel I
	RHO (I)	Floating Point	Bottom reflectance in channel I
	TAU (I)	Floating Point	Atmospheric Transmissivity in channel I
	EK (I)	Floating Point	Scanner sensitivity constant in channel I
	H (I)	Floating Point	Solar irradiance at surface in channel I
	SDA	Floating Point	Solar-zenith angle
	DEL	Floating Point	Angular separation of points along scan line
	XMID	Integer	Point number of nadir
	VF	Integer	Amplitude of fluctuations in deep-water signal
	EDITCH	Integer	Channel No. used for editing out land
	LO	Integer	Minimum signal observed over water in channel EDITCH
	HI	Integer	Maximum signal observed over water in channel EDITCH

TABLE A-2. LISTING OF DEPTH1 PROGRAM

```
 EXTERNAL FUNCTION DEPTH1.

*****************************************************************
*                                                               *
*  WATER DEPTH SUBROUTINE PACKAGE -- 11 MARCH 1973 -- MFG       *
*                                                               *
*    THIS PACKAGE IS DESIGNED TO CALCULATE THE DEPTH OF         *
*    SHALLOW WATER AREAS BASED ON THE DIFFERENCE BETWEEN        *
*    THE REFLECTANCES OR RADIANCES OVER SHALLOW AND OVER        *
*    DEEP WATER AREAS.                                          *
*                                                               *
*****************************************************************


  NORMAL MODE IS INTEGER
  REFERENCES ON

  ERASABLE SKP2(225), OUNIT, OREEL, OFILE, OLINE, IWRITE, OCHAN,
1   ONWDS, PROG, MODE1, MODE2, UNIT, CALINE, OLINC, NSA, NSB,
2   KS, NA, NB, KP, ID(1), IFLAG, IPACK, RESERV(4), QFACTR(49),
3   QTITL2(19), QTITLE(19), QLIST(19), QSPARE(46), QFLAG,
4   QDANG, QBANG, QKP, QNA, QNSS, QNCHAN, QMODE, QRECA, QRECD,
5   OFILE, OREEL, QNWRDS
  ERASABLE DATA(423), ITEST, USTART, DSTART, NV, NX, NC, L, IP,
1   IOP, NOP, NEXT, START, READT, READL, READP, LABEL,
2   EXTRA(20), DATUM(24), ICODE(24), ICHAN(24), COEF(1)


 ** DIMENSION AND MODE DECLARATIONS **

  DIMENSION DEEP(24)
  DIMENSION ACOEF(400*12)
  DIMENSION IA(2),PAIRS(18*2),PMODE(1),RET(24),MAX(24)
  FLOATING POINT F(1000),H(24),VSS(24),ALPHA(24),TAU(24),G(18),A(18*2),
1               RHO(24),FMAX(24),RHOSS(24),QFACTR
  FLOATING POINT QBANG,QDANG,SDA,DEL,W,X,P180,C51
  FLOATING POINT SQRT.,COS.,ELOG.
  FLOATING POINT EK(24)
  BOOLEAN BRMODE

 ** VECTOR VALUES **

  VECTOR VALUES EK...EK(24)=1.0
  VECTOR VALUES C51=51.0
  VECTOR VALUES P180=0.01745329
  VECTOR VALUES RERR=$H'ORETURN CODE OF',I4,H' FROM COEFFICIENT FILE READ
1  ',I1*$
  WHENEVER NEXT.G.3, FUNCTION RETURN
  TRANSFER TO STEP(NEXT)

 ** STEP 1 - PROGRAM INITIALIZATION **
```

```
STEP(1)     CBIN1 = -1
            ZERO.(CUNIT,EDITCH,HI,LO)
            SPRAY.(1., TAU(1)...TAU(24))
            SDA = -999.
            VF=1
            LINK.(DEP1.)
            READ AND PRINT DATA
            FUNCTION RETURN

           ** STEP 2 - INPUT COEFFICIENT FILE, IF NECESSARY  **
           **         - INPUT PROGRAM VARIABLES AND CALCULATE **
           **           NECESSARY ARRAYS                      **

STEP(2)     ZERO.(CBIN,CFILE,XMID,DEL,NPAIRS,PAIRS...PAIRS(36),LCTR)
            PMODE = $RADIAN$
            PROG = $DEPTH$
            ZERO.(COEFSW,DEEP(1)...DEEP(24))
            READ AND PRINT DATA
            WHENEVER COEFSW.NE.0, TRANSFER TO BR0
            WHENEVER TFLAG.E.0, TRANSFER TO BR1
           ** READ IN A COEFFICIENT FILE **
            WHENEVER CBIN1.E.-1.AND.CBIN.E.0
              PRINT FORMAT $H*ONO COEFFICIENT TAPE SPECIFIED**$
ERR           ERROR.
            END OF CONDITIONAL
           ** TAPE ACTION **
            WHENEVER CBIN.E.CBIN1
              REWIND TAPE CUNIT
            OTHERWISE
              MOUNT.(CBIN,CUNIT,$OUT$)
              CBIN1 = CBIN
            END OF CONDITIONAL
            SKIP.(CFILE-1,0,CUNIT)
           ** READ FIRST RECORD OF COEFFICIENT FILE **
            RBIN.(CUNIT,IA(2),3)
            RC = RCHECK.(0)
            WHENEVER RC.NE.0
              PRINT FORMAT RERR,RC,1
              TRANSFER TO ERR
            END OF CONDITIONAL
           ** CHECK FOR ADDITIVE COEFFICIENTS **
            N = ONSS * ONCHAN
            WHENEVER IA.E.0
              WHENEVER N.NE.(IA(1)*IA(2))
                PRINT FORMAT $H*OINCONSISTENCY BETWEEN COEFFICIENT FILE AND DATA F
          1 ILE*/H*0** COEF FILE ** NSS =*,I5,S5,H*NCHAN =*,I5/H* ** DATA
          2  FILE ** NSS =*,I5,S5,H*NCHAN =*,I5/*$,IA(1),IA(2),ONSS,
          3       ONCHAN
                  TRANSFER TO ERR
                END OF CONDITIONAL
              OTHERWISE
                PRINT COMMENT $ONON-ADDITIVE COEFFICIENT FILE$
                TRANSFER TO ERR
              END OF CONDITIONAL
           ** READ COEFFICIENT RECORD **
            RBIN.(CUNIT,ACOEF(N),N)
            RC = RCHECK.(0)
            WHENEVER RC.NE.0
              PRINT FORMAT RERR,RC,2
```

```
              TRANSFER TO ERR
            END OF CONDITIONAL


BR0         SETDIM.(ACOEF,1...GNSS,1...GNCHAN)
            WHENEVER COEFSW.NE.0
              THROUGH CLOOP1, FOR I=1,1,I.G.GNSS
              (J=1,1,J.G.GNCHAN, ACOEF(I,J) = -DEEP(J) )
CLOOP1        CONTINUE
            END OF CONDITIONAL

           ** CHECK IF NEW F-FUNCTION MUST BE COMPUTED **

            WHENEVER IFLAG.E.0.AND.XMID.E.0, TRANSFER TO BR1
           ** COMPUTE F-FUNCTION **
            WHENEVER SDA.L.-360.
              PRINT COMMENT $0SUN DEPRESSION ANGLE NOT SPECIFIED FOR NEW
          1 DATA FILE$
              TRANSFER TO ERR
            END OF CONDITIONAL
            WHENEVER DEL.E.0
              WHENEVER GDANG.E.0.
                PRINT FORMAT $H'0UNABLE TO COMPUTE F-FUNCTIONS'*$
                TRANSFER TO ERR
              END OF CONDITIONAL
            OTHERWISE
              GDANG = DEL * P180
              GBANG = -((XMID - GNA)/GKP) * GDANG
            END OF CONDITIONAL
            G = 1. / COS.(SDA*P180)
            X = GBANG
            THROUGH LOOP1,FOR I=1,1,I.G.GNSS
            F(I) = 1. / (1./COS.(X) + G )
LOOP1       X = X + GDANG
            PRINT RESULTS F(1)...F(GNSS)
           ** CHECK PAIRS FOR CONSISTENCY **
BR1         THROUGH LOOP2,FOR I=1,1,I.G.NPAIRS
            WHENEVER PAIRS(I,1).G.GNCHAN.OR.PAIRS(I,2).G.GNCHAN
              PRINT COMMENT $0CHANNEL-PAIR COMPONENT GREATER THAN NUMBER
          1 OF CHANNELS ON INPUT TAPE$
              TRANSFER TO ERR
            END OF CONDITIONAL
           ** COMPUTE G-FUNCTION FOR EACH PAIR **
LOOP2       G(I) = 1. / (ALPHA(PAIRS(I,1)) - ALPHA(PAIRS(I,2)))
            PRINT RESULTS G(I)
           ** RADIANCE MODE CALCULATIONS **
            WHENEVER PMODE.E.$RADIAN$
              THROUGH LOOP3,FOR K=1,1,K.G.NPAIRS
              I = PAIRS(K,1)
              J = PAIRS(K,2)
              Q = (RHO(I)*H(I)*TAU(I)) / (RHO(J)*H(J)*TAU(J))*EK(I)/EK(J)
LOOP3         A(K) = ELOG.(Q)
            PRINT RESULTS Q,A(I)
              BRMODE = 1B

           ** REFLECTANCE MODE CALCULATIONS **
            OTHERWISE
           ** CHECK VALIDITY OF SUN SENSOR REGION **
              WHENEVER NAS.G.NBS
                PRINT FORMAT $H'0NAS GREATER THAN NBS ** NAS =',I4,H' NBS =',I4*$,
```

```
     1                    NAS,NBS
           TRANSFER TO ERR
         OR WHENEVER NAS.G.(QNA+(QNSS-1)*QKP)
           PRINT FORMAT $H'0SUN SENSOR REGION NOT AVAILABLE'*$
           TRANSFER TO ERR
         END OF CONDITIONAL
         NAS1 = (NAS - QNA)/QKP + 1
         I = (QNA+(QNSS-1)*QKP)
         WHENEVER NBS.G.I , NBS = 1
         NBS1 = (NBS - QNA)/QKP + 1
         BRMODE = QB
       END OF CONDITIONAL
       BP1 = (NA - QNA) / QKP + 1
       QBP = KP / QKP
       (I=1,1,I.G.NC, QFACTR(I) = 1/51.0,QFACTR(I+25)=-1./51.0)
       QFLAG = 2
       FUNCTION RETURN

      ** STEP 3 - LINE OPERATIONS **

STEP(3)  K = QSTART + 8
       LCTR = LCTR + 1
       BP = BP1
      ** CALCULATE A-VECTOR FROM SUN SENSOR REGION, **
      ** IF REFLECTANCE MODE                       **
       WHENEVER BRMODE, TRANSFER TO BR2
       SPREAD.(-1,MAX(1)...MAX(QNCHAN))
       THROUGH LOOP4,FOR I=NAS1,1,I.G.NBS1
       VAL.(DATA(K),I)
       THROUGH LOOP4,FOR J=1,1,J.G.QNCHAN
       WHENEVER RET(I).G.MAX(I), MAX(I) = RET(I)
LOOP4  CONTINUE
       (I=1,1,I.G.QNCHAN, FMAX(I) = MAX(I))
       EXPSMT.(FMAX,VSS,QNCHAN)
       THROUGH LOOP5,FOR N=1,1,N.G.NPAIRS
       I = PAIRS(N,1)
       J = PAIRS(N,2)
       Q = (RHO(I)*RHOSS(I)*VSS(I)*TAU(I)*TAU(I)) /
     1     (RHO(J)*RHOSS(J)*VSS(J)*TAU(J)*TAU(J))
LOOP5  A(N) = ELOG.(Q)
BR2    FUNCTION RETURN


       INTERNAL FUNCTION DEP1.
       FLOATING POINT Z(18),MEAN,SDEV
       I = DATUM(EDITCH)
       WHENEVER I.G.HI.OR.I.L.LO
         ZERO.(DATUM(1)...DATUM(NC))
         TRANSFER TO DBR1
       END OF CONDITIONAL
       SDEV = 0.
       MEAN = 0.
       THROUGH ILOOP,FOR M=1,1,M.G.NPAIRS
       I = PAIRS(M,1)
       J = PAIRS(M,2)
       V2 = DATUM(J) + ACOEF(BP,J)
       V1 = DATUM(I) + ACOEF(BP,I)
      **VF IS LEVEL OF FLUCTUATIONS IN DEEP WATER VOLTAGE**
       WHENEVER V2.L.VF.OR.V1.L.VF
         Z(M) = 10.1
```

```
                OTHERWISE
                X = V2
                X = X / V1
                  Q = ELOG.(X)
                  Z(M) = F(BP) * G(M) * ( A(M) + Q )
                END OF CONDITIONAL
                WHENEVER Z(M).L.0., Z(M) = 0
ILOOP           MEAN = MEAN + Z(M)
                MEAN = MEAN / NPAIRS
               ** CALCULATE STANDARD DEVIATION,WHILE SCALING DATA **
                THROUGH ILOOP1,FOR M=1,1,M.G.NPAIRS
                Q = Z(M) - MEAN
                SDEV = SDEV + Q * Q
ILOOP1          DATUM(M) = Z(M) * C51 + 1.
                WHENEVER NPAIRS.E.1
                  DATUM(3) = 0
                OTHERWISE
                  SDEV = SQRT.(SDEV/(NPAIRS-1))
                  DATUM(NPAIRS+2) = SDEV * C51
                END OF CONDITIONAL
                  DATUM(NPAIRS+1) = MEAN * C51
                THROUGH ILOOP2,FOR I=1,1,I.G.NC
                WHENEVER DATUM(I).G.511,DATUM(I) = 511
ILOOP2          CONTINUE
DBR1            BP = BP + DBP
                FUNCTION RETURN
                END OF FUNCTION


                INTERNAL FUNCTION VAL.(ARRAY,XX)
                THROUGH LOOP,FOR II=0,1,II.E.QNCHAN
                YY = (XX-1)*QNCHAN + II
                WORD = YY / 4
                DISP = (3-(YY-WORD*4))*9
LOOP            RET(II+1) = (ARRAY(WORD).RS.DISP).A.511
                FUNCTION RETURN
                END OF FUNCTION


                INTERNAL FUNCTION EXPSMT.(IN,OUT,NN)
                FLOATING POINT IN,OUT,ZZ,Z1
                WHENEVER LCTR.G.10
                  TRANSFER TO ELOOP
                OR WHENEVER LCTR.E.10
                  ZZ = 0.1
                  Z1 = 0.9
                OR WHENEVER LCTR.G.1
                  ZZ = 1./LCTR
                  Z1 = 1. - ZZ
                OTHERWISE
                  ZZ = 0.
                  Z1 = 1.
                END OF CONDITIONAL
ELOOP           (I = 1,1,I.G.NN, OUT(I) = OUT(I)*ZZ + IN(I)*Z1 )
                FUNCTION RETURN
                END OF FUNCTION


                END OF FUNCTION
```

Appendix B
COMPUTER PROGRAM FOR OPTIMUM DECISION-BOUNDARY METHOD

A computer program also was written to implement the method of depth calculation discussed in Section 3.4. This program can use any number of input channels and writes out the depth values at each point on a single-channel output tape. The input data include the signal at the known depth, which may be zero (using the highest signal observed at the water's edge).

The input variables are summarized in Table B-1, and the computer coding is listed in Table B-2.

TABLE B-1. VARIABLES FOR DEPTH2 PROGRAM

Card 1:

Input Variables	Mode	Description
NV	Integer	No. of channels on input tape
NCHAN	Integer	No. of channels used in the depth calculation (NCHAN ≤ NV)
CHAN (I)	Integer	Channel number used (I=1, . . . N CHAN)

Card 2
(process variables):

same as for DEPTH1

Card 3:

ALPHA(I)	Floating Point	Water-attenuation coefficient in CHAN(I)
DEEP(I)	Integer	Deep-water signal in CHAN(I)
VREF(I)	Integer	Reference signal in CHAN(I)
ZREF	Floating Point	Water depth where reference signal is measured
SDA	Floating Point	Solar-zenith angle
EDITCH	Integer	Same as in DEPTH1
LO	Integer	Same as in DEPTH1
HI	Integer	Same as in DEPTH1

Notice that this program does not require a knowledge of the bottom reflectance, sensitivity constants, solar irradiance, or atmospheric transmissivity. All the necessary information is contained in the reference signal VREF(I).

Scan-angle variations have been neglected, eliminating the input variables DEL and XMID.

If there are variations in bottom reflectance in the scene, the depth values will be in error by an additive factor for the areas where the bottom reflectance differs from that where VREF(I) was measured. In some cases, however, it might be possible to choose a set of channels to minimize or eliminate this error.

TABLE B-2. LISTING OF DEPTH2 PROGRAM

```
          EXTERNAL FUNCTION DEPTH2.

          NORMAL MODE IS INTEGER
          REFERENCES ON

          ERASABLE SKP2(225), OUNIT, OREEL, OFILE, OLINE, TWRITE, OCHAN,
         1   ONWDS, PROG, MODE1, MODE2, UNIT, CALINE, COLINE, NSA, NSB,
         2   KS, NA, NB, KP, ID(1), TFLAG, IPACK, RESERV(4), QFACTR(49),
         3   QTITL2(19), QTITLE(19), QLIST(19), QSPARE(46), QFLAG,
         4   QDANG, QBANG, QKP, QNA, QNSS, QNCHAN, QMODE, QRECA, QRECD,
         5   QFILE, QREEL, QNWRDS
          ERASABLE DATA(423), ITEST, QSTART, DSTART, NV, NX, NC, L, IP,
         1   IGP, NOP, NEXT, START, READT, READL, READP, LABEL,
         2   EXTRA(20), DATUM(24), ICODE(24), ICHAN(24), COEF(1)


          DIMENSION CHAN(24),VREF(24),DEEP(24)
          FLOATING POINT ALPHA(24),QFACTR,SDA,X,P180,C51
          FLOATING POINT Z,ZREF,ZMAX,C,V
          FLOATING POINT SQRT.,COS.,ELOG.

          VECTOR VALUES C51=50.0
          VECTOR VALUES P180=0.01745329
          WHENEVER NEXT.G.2, FUNCTION RETURN
          TRANSFER TO STEP(NEXT)

STEP(1)   NC=1
          LINK.(DEP2.)
          READ AND PRINT DATA  NV,NCHAN,CHAN(1)...CHAN(NCHAN)
          FUNCTION RETURN

STEP(2)   ZERO.(DEEP(1)...DEEP(24))
          ZERO.(EDITCH,LO,HI)
          ZREF=0.
          READ AND PRINT DATA  ALPHA(I),DEEP(I),VREF(I),ZREF,SDA,EDITCH,LO,HI
          C=0.
          THROUGH DRL1, FOR I=1,1,I.G.NCHAN
DRL1      C=C+ALPHA(I)*ALPHA(I)
          C=C*(1.+1./COS.(SDA*P180))
          ZMAX=ZREF
          THROUGH DRL2, FOR I=1,1,I.G.NCHAN
          V=VREF(I)-DEEP(I)
DRL2      ZMAX=ZMAX+ALPHA(I)*ELOG.(V)/C
          PRINT RESULTS ZMAX
          QFACTR(1)=1./C51
          QFACTR(26)=0.
          QFLAG=2
          FUNCTION RETURN

          INTERNAL FUNCTION DEP2.
          I = DATUM(EDITCH)
          WHENEVER I.G.HI.OR.I.L.LO
          DATUM(1)=511
```

```
            TRANSFER TO DRL4
            END OF CONDITIONAL
            Z=ZMAX
            THROUGH DRL3, FOR I=1,1,I.G.NCHAN
            V=DATUM(CHAN(I))-DEEP(I)
            WHENEVER V.LE.0.,TRANSFER TO DRL3
            X=ELOG.(V)
            Z=Z-ALPHA(I)*X/C
DRL3        CONTINUE
            WHENEVER Z.L.0., Z=0.
            DATUM(1)=Z*C51+0.5
            WHENEVER DATUM(1).G.500,DATUM(1) = 500
DRL4        CONTINUE
            FUNCTION RETURN
            END OF FUNCTION

            END OF FUNCTION
```

REFERENCES

1. John T. Smith, Jr., Color - A New Dimension in Photogrammetry, Photogrammetric Engineering, Vol. XXIX, No. 6, November 1963, pp. 999-1013.
2. Lawrence W. Swanson, Aerial Photography and Photogrammetry in the Coast and Geodetic Survey, Photogrammetric Engineering, Vol. XXX, No. 5, September 1964, pp. 699-726.
3. Edward L. Geary, Coastal Hydrography, Photogrammetric Engineering, Vol. XXXIV, No. 1, January 1968, pp. 44-50.
4. W. L. Brown, F. C. Polcyn, A. N. Sellman, and S. R. Stewart, Water-Depth Measurement by Wave Refraction and Multispectral Techniques, Report No. 31650-31-T, Willow Run Laboratories, Ann Arbor, August 1971.
5. G. J. Zissis et al., Design of a Study to Evaluate Benefits and Costs of Data from the First Earth Resources Technology Satellite (ERTS-A), Report No. 11215-1-F, Willow Run Laboratories, Ann Arbor, July 1972.
6. ERTS Data Users Handbook, Goddard Space Flight Center, National Aeronautics and Space Administration, Greenbelt, Maryland, 1972.
7. F. C. Polcyn and R. A. Rollin, Remote Sensing Techniques for the Location and Measurement of Shallow Water Features, Report No. 8973-10-P, Willow Run Laboratories of the Institute of Science and Technology, The University of Michigan, Ann Arbor, January 1969.

DISTRIBUTION LIST

NASA/Goddard Space Flight Center
Greenbelt, Maryland 20771

ATTN: Scientific Investigations
Support, Code 902.6 (10)